

**COPPER OXIDE NANOPARTICLES SYNTHESIS AND  
APPLICATIONS**

A DISSERTATION

SUBMITTED IN PARTIAL FULFILLMENT OF THE REQUIREMENTS FOR THE  
AWARD OF THE DEGREE

OF

**MASTER OF SCIENCE**

IN

**PHYSICS**

Submitted by:

**ANKITA DAHIYA**

**(2K22/MSCPHY/04)**

**BHARAT BHUSHAN**

**(2K22/MSCPHY/07)**

Under the supervision of

**DR. MOHAN SINGH MEHATA**

(Assistant Professor)



**DEPARTMENT OF APPLIED PHYSICS**

**DELHI TECHNOLOGICAL UNIVERSITY**

(Formerly Delhi College of Engineering)

Bawana Road, Delhi-110042

JUNE, 2024

## CANDIDATE'S DECLARATION

We, ANKITA DAHIYA, Roll No. 2K22/MSCPHY/04 and BHARAT BHUSHAN, Roll No. 2K22/MSCPHY/07 students of M.Sc. Physics hereby declare that the project Dissertation titled "**Copper Oxide Nanoparticles Synthesis and Applications**" which is submitted by us to the Department of Applied Physics, Delhi Technological University, Delhi in partial fulfilment of the requirement for the award of the degree of Master of Science, is original and not copied from any source without proper citation. This work has not previously formed the basis for the award of any Degree, Diploma Associateship, Fellowship or other similar title or recognition.

- The work has been accepted in peer reviewed Scopus indexed conference with the following details:

**Title of the paper:** "Surfactant Free and Facile Synthesis of Cuboidal Shaped Nanoparticles for Acetone Sensing".

**Authors Names (In sequence as per Research Paper):** Bharat Bhushan, Ankita Dahiya, Vinay Kumar Yadav, Gagan Sharma, Mohan Singh Mehata.

**Name of the Conference:** International Conference on Atomic, Molecular, Material, Nano, and Optical Physics with Applications – 2023

**Conference Dates with venue:** December 20<sup>th</sup> – 22<sup>th</sup> at Delhi Technological University, Delhi.

**Have you registered for the conference:** Yes

**Status of Paper:** Accepted

**Date of Communication:** 25 April 2024

**Date of Acceptance:** 30 May 2024

**Date of paper publication:** Yet to be published

*Ankita*

*Bharat Bhushan*

Place: Delhi

Ankita Dahiya

Bharat Bhushan

Date: June 7, 2024

(2K22/MSCPHY/04)

(2K22/MSCPHY/07)

**DEPARTMENT OF APPLIED PHYSICS**

**DELHI TECHNOLOGICAL UNIVERSITY**

(Formerly Delhi College of Engineering)


Bawana Road, Delhi-110042

**CERTIFICATE**

I, hereby certify that the Project Dissertation titled "**Copper Oxide Nanoparticles Synthesis and Applications**" which is submitted by **ANKITA DAHIYA**, Roll No. **2K22/MSCPHY/04** and **BHARAT BHUSHAN**, Roll No. **2K22/MSCPHY/07**, Department of Applied Physics, Delhi Technological University, Delhi in partial fulfilment of the requirement for the award of the degree of Master of Science, is a record of the project work carried out by the students under my supervision. To the best of my knowledge this work has not been submitted in part or full for any Degree or Diploma to this University or elsewhere.

Place: Delhi

Date: 07/06/2024.

  
9/6/2024  
Dr. Mohan Singh Mehata

## ACKNOWLEDGEMENT

I would like to express my indebtedness and deepest sense of regard to my supervisor, **Dr. Mohan Singh Mehata**, Assistant Professor, Department of Applied Physics, Delhi Technological University for providing his incessant expertise, inspiration, encouragement, suggestions, and this opportunity to work under his guidance. I am thankful for the constant help provided at every step of this project by **Mr. Vinay Yadav** and all other lab members of Laser Spectroscopy Laboratory, Department of Applied Physics, Delhi Technological University. I am also thankful to my family and colleagues for their invaluable support, care and patience during this project. Lastly, I would thank Delhi Technological University for providing such a wonderful opportunity of working on this project.

## **ABSTRACT**

In this work, the CuO nanoparticles were effectively synthesized by the conventional hydrothermal method at different temperatures and by using different precursors. A strong base was used for the precipitation of nanoparticles resulting in no templating agent being needed for the process to occur. Three different samples were prepared using copper chloride and copper nitrate as precursors at 150 °C and 180 °C. Different characterization techniques were used to examine which sample is best suited for gas sensing applications. Crystallography and morphological analysis suggested that sample prepared at 150 °C using copper nitrate as precursor shows good sensitivity compared to other samples. Further all other characterizations are performed for this sample. X-ray diffraction pattern confirms nanoparticles have a crystallite size of 44 nm with a monoclinic phase of CuO. Highly dense and uniformly distributed particles with lower particle size can be seen by FESEM images. Bond vibration frequencies were used to detect the presence of Cu-O bond in the sample using FTIR spectroscopy. Compositional analysis was done with EDX spectroscopy. The photoluminescence (PL) analysis was performed and a peak maximum was observed at 417 nm might be due to the presence of defect states. Sensitivity analysis of acetone depicts CuO has a low response and recovery time and is highly sensitive to acetone gas. Thus, a low-cost and efficient volatile gas sensor with a sustainable approach is proposed.

## TABLE OF CONTENT

|   |      |
|---|------|
| <b>Candidate's Declaration</b>                      | I    |
| <b>Certificate</b>                                  | ii   |
| <b>Acknowledgement</b>                              | iii  |
| <b>Abstract</b>                                     | iv   |
| <b>Table of Content</b>                             | v    |
| <b>List of Figures</b>                              | vii  |
| <b>List of Tables</b>                               | viii |
| <b>List of Symbols, Abbreviations</b>               | ix   |
| 1. Introduction                                     | 1    |
| 1.1. Nanotechnology                                 | 1    |
| 1.2. Literature Review                              | 2    |
| 1.2.1. Synthesis Method of Nanoparticles            | 2    |
| 1.2.2. Copper Oxide                                 | 2    |
| 1.2.3. Copper Oxide Nanoparticles                   | 3    |
| 1.2.4. Applications of Copper Oxide Nanoparticles   | 4    |
| 2. Nanomaterials and Synthesis Process              | 6    |
| 2.1. Nanomaterials                                  | 6    |
| 2.2. Synthesis Approach                             | 7    |
| 2.2.1. Synthesis Method for Nanomaterials Synthesis | 8    |
| 3. Hydrothermal Synthesis of CuO Nanoparticles      | 10   |
| 3.1. Hydrothermal Method                            | 10   |
| 3.2. Synthesis Process                              | 10   |
| 3.2.1. Materials                                    | 10   |
| 3.2.2. Sample Preparation                           | 10   |
| 3.2.3. Film Deposition and Gas Sensing Measurement  | 11   |
| 3.2.4. Synthesis Steps                              | 12   |
| 4. Results and Discussion                           | 13   |
| 4.1. Crystallography Analysis                       | 13   |
| 4.2. Morphological Analysis                         | 15   |

|                                      |    |
|--------------------------------------|----|
| 4.3. EDX Analysis                    | 17 |
| 4.4. FTIR Analysis                   | 21 |
| 4.5. Uv-vis Analysis                 | 22 |
| 4.6. Photoluminescence Analysis      | 24 |
| 5. Application as Acetone Gas Sensor | 26 |
| 6. Conclusion                        | 28 |
| Bibliography                         | 29 |
| Plagiarism Report                    | 35 |
| Conference Record                    | 39 |
| Accepted Paper                       | 43 |

## LIST OF FIGURES

**Figure 2.1:** Nanomaterials classification based on dimensionality.

**Figure 2.2:** Bottom-up and top-down approach for synthesis of nanomaterials.

**Figure 3.1:** Schematic representation of synthesis process of CuO nanoparticles.

**Figure 4.1:** XRD pattern of sample S1 along with JCPDS file.

**Figure 4.2:** XRD pattern of sample S2 along with JCPDS file.

**Figure 4.3:** XRD pattern of sample S3 along with JCPDS file.

**Figure 4.4:** Fe-sem images of sample S1 synthesized using precursor Copper chloride (a) 1  $\mu\text{m}$  and (b) 200 nm.

**Figure 4.5:** Fe-sem images of sample S2 synthesized using precursor Copper nitrate (a) 1  $\mu\text{m}$  and (b) 200 nm.

**Figure 4.6:** Fe-sem images of sample S3 synthesized using precursor Copper nitrate (a) 2  $\mu\text{m}$  and (b) 200 nm.

**Figure 4.7:** EDX spectra of sample S1 synthesized using copper chloride as precursor.

**Figure 4.8:** EDX spectra of sample S2 synthesized using copper nitrate as precursor.

**Figure 4.9:** EDX spectra of sample S3 synthesized using copper nitrate as precursor.

**Figure 4.10:** FTIR spectrum of Sample S2 synthesized using copper nitrate as precursor.

**Figure 4.11:** Absorption spectra of CuO synthesized at 150  $^{\circ}\text{C}$  using copper nitrate as precursor i.e. sample S2.

**Figure 4.12:** Tauc's plot for indirect bandgap of synthesized CuO nanoparticles sample S2.

**Figure 4.13:** Emission spectra of CuO nanoparticles synthesized using copper nitrate as precursor at 150  $^{\circ}\text{C}$ .

**Figure 5.1:** Variation of resistance (Ohm) with time for different cycles. Response recovery plot of CuO as acetone gas sensor at 300  $^{\circ}\text{C}$ .



## LIST OF TABLES

**Table 4.1:** Composition table showing atomic and weight percentage of elements in sample S1.

**Table 4.2:** Composition table showing atomic and weight percentage of elements in sample S2.

**Table 4.3:** Composition table showing atomic and weight percentage of elements in sample S3.

## LIST OF SYMBOLS, ABBREVIATIONS

|        |   |
|--------|---|
| NPs    | Nanoparticles                                   |
| nm     | Nano meters                                     |
| CuO    | Copper Oxide                                    |
| XRD    | X-ray diffraction                               |
| Fe-sem | Field emission scanning electron microscopy     |
| EDX    | Energy dispersive X-ray spectroscopy            |
| FTIR   | Fourier transform infrared spectroscopy         |
| PL     | Photoluminescence                               |
| UV     | Ultraviolet – Visible                           |
| S      | Sensitivity                                     |
| JCPDS  | Joint Committee on Powder Diffraction Standards |

# CHAPTER -1

## INTRODUCTION

### 1.1. NANOTECHNOLOGY

Nanotechnology is a multidisciplinary field at the intersection of science, engineering, and technology, focusing on manipulating substance in the nanoscale, usually found in the 1–100 nm range. Materials have special qualities and behaviour at this small scale, distinct from their bulk counterparts. The ability to understand, control, and exploit these phenomena has given rise to groundbreaking applications across various fields such as cancer therapy [1], wastewater treatment [2], medicine delivery [3], and solar energy converters [4]. Because of the remarkable advancements in nanotechnology in recent years, researchers have become more interested in finding dependable and effective ways to produce nanomaterials between one and one hundred nanometres [5]. Nanomaterials are of increasing interest due to their unique optoelectronic, physicochemical, and magnetic capabilities when compared to their bulk form [6]. Carbon-based, metallic, polymeric, semiconductor quantum dot, and magnetic nanoparticles are some of the main types of nanostructures with biological relevance [7]. For biological identification and detection, quantum dots are useful due to their size-dependent fluorescence properties. It has been possible to sort cells using magnetic nanoparticles [8].

Many scientific and industrial uses can be found for metal oxide nanoparticles, making them a versatile material [9]. A lot of material scientist are still facing issues of synthesizing cost effective and high-quality nanoparticles with proper phase production, chemical purity and a controlled agglomeration of particles [10]. Research on synthetic technique and sensor device technology has shown a great deal of interest in nanomaterials [11]. The remarkable size-dependent chemical and physical features of nanostructured materials, along with their potential technological applications, have received significant attention in the world of science for their research and development [12].

Recently, copper-based nanomaterials have drawn interest of researchers due to their applicability in superconductors, optoelectronic devices, and catalysis [13]. An essential

functional material is the nanostructured copper oxide (CuO), the p type semiconductor. It is used in semiconductors, varistor (variable resistor), solar energy conversion, magnetic storage equipment, detectors for gases, and electronics, and catalysis. It has a direct energy band gap and special optical and magnetic characteristics [14]. For this reason, it has been investigated together with other copper oxides, specifically regarding its potential uses as a photothermally active and photoconductive substance [15].

## **1.2. LITERATURE REVIEW**

### **1.2.1. SYNTHESIS METHODS OF NANOPARTICLES**

A large-scale synthesis of different nanomaterials is accomplished by the application of several physical and chemical techniques [16]. Chemical processes like chemical bath deposition [17], microwave assisted [18], hydrothermal [19], sol-gel [20], sonochemical approach [21], electrochemical technique [22], and precipitation [23] and microwave assisted synthesis [24] using harsh reducing agents, organic solvents, and toxic compounds along with the production of harmful by-products [25] are the main techniques through the chemical approach. High energy and time are required for physical synthesis techniques such as vacuum vapor deposition [26], mechanical milling [27], pulsed laser [28], gamma radiation [29], and plasma [30]. Adopting a successful and ecologically friendly strategy is required for synthesizing nanomaterials by taking into account the limits of chemical and physical processes [31].

### **1.2.2. COPPER OXIDE (CuO)**

Due to its strong thermal and electrical conductivities, copper is a valuable material. CuO is the formula for the inorganic compound copper oxide (CuO). It is black solid powder having two different forms CuO and Cu<sub>2</sub>O. CuO is referred to as tenorite and paramelaconite in the mineral world. It is an outcome of the mining of copper and the starting point for numerous other goods and chemical compounds that contain copper. By using pyrometallurgy to separate copper from ores, it is manufactured on a large scale. The equivalent copper (II) salts are produced when copper (II) oxide dissolved in mineral acids. A mild explosive, not an incendiary, is produced when cupric oxide is added to

thermite instead of iron oxide [32]. An important class of semiconductors are the transition metal oxides. Cu and its oxides are among the many semiconductors that have gained a lot of interest in practical applications because of its optical, electrical conducting, and catalytic properties [33]. The monoclinic crystal structure includes copper (II) oxide. Each atom in the compound CuO has four nearest neighbours of the same kind, with a narrow band gap, copper (II) oxide is a p-type semiconductor. Dry cell batteries can be made from cupric oxide. It might also be utilized as the cathode in wet cell batteries, where the anode would be lithium and the electrolyte would be a mixture of dioxolane and lithium perchlorate [34].

### **1.2.3. COPPER OXIDE NANOPARTICLES (CuO NPs)**

Recent years have seen a significant increase in interest in nanocrystalline semi-conductor particles due to their unique characteristics, which include a high surface-to-volume ratio [35]. Some of the distinctive characteristics of nanoparticles can be credited to their enormous surface to volume ratio. An essential class of semiconductors are the oxides of transition metals. Cu and its oxides are among the numerous semiconductors that have governed a lot of interest in fundamental research as well as technical application due to their catalytic, optical, and electrical conducting capabilities [36]. Covalent semiconductor copper (II) oxide has a comparatively small band gap. Strong electron correlation in this narrow band semiconductor complicates CuO's optical characteristics [37]. Copper oxide is (CuO) a semiconductor with a monoclinic structure [38]. CuO crystal also possesses photoconductive and photocatalytic properties. CuO has several uses because it is less expensive than silver, blends nicely with polymers, and has physical and chemical properties that are generally stable. Given their ability to be manufactured with very large surface areas and peculiar crystal morphologies, highly ionic nanoparticulate metal oxides, like CuO, are considered to have potential use as antibacterial agents [39]. Furthermore, in addition to their size, these nanoparticles' structure, shape, size distribution, and chemical and physical environments all these parameters affect their catalytic activity. Controlling the size and size distribution is therefore a crucial task. Generally, by altering the synthesis techniques, reaction conditions, reducing agents, and stabilizers allows for precise control over shape, size, and size distribution [40].

#### 1.2.4. APPLICATIONS OF COPPER OXIDE NANOPARTICLES

Copper and its oxides are among the numerous semiconductors that have attracted a lot of interest in fundamental research as well as technical application due to their catalytic, optical, and electrical conducting capabilities [41].

Alcohols are synthesized using copper monoxide as a catalyst. It has been observed that exposing CuO to high-energy particle radiation causes a noticeable acceleration of catalysed processes. Due to their effectiveness as nanofluids in heat transfer applications, copper oxide nanoparticles are particularly interesting among the oxides of transition metals. According to reports, adding 4% of CuO increases water's thermal conductivity by 20% [42].

The strong electrical and thermal conductivities of copper make it a valuable material. Promising materials for magnetic storage, gas sensors, catalysis, varistors, semiconductors, and solar energy conversion include CuO, a p-type semiconductor with narrow band gaps [43].

When organic pollutants are exposed to semiconductor photocatalysts, strong light sources, and oxidising agents like oxygen or air, the pollutants are broken down by the photocatalysts. Potential interactions with organic pollutants become possible as a result. The absorption of photons with energy less than band gap energy frequently leads to heat dissipation. When the photocatalyst is adequately lit, an electron forms in the conduction band and a hole develops in valence band. Pollutants are directly oxidized by holes, oxygen absorbed on photocatalyst is decreased by the electron in the conduction band [44].

Humans efficiently metabolize copper, which is a trace metal that is necessary for the healthy operation of numerous tissues, including the skin, heart, neurological system, and immune system. Since copper (II) oxide has a nearly non-existent bioavailability, it should be taken when there is a copper shortage, particularly when combined with zinc

or molybdenum in a multivitamin. Copper is eliminated from the body by an excessive intake of zinc or molybdenum.

Copper oxide is a harmless form of copper that is used in over-the-counter medications and vitamin supplements. Since copper oxide has antibacterial and cosmetic qualities, it is also utilized in consumer goods like socks and pillowcases. Dermal sensitivity to copper is thought to be incredibly unlikely. CuO is utilized as a gas sensing material to identify poisonous, flammable, and polluting gases due to its inexpensive cost. Oxide semiconductors' gas sensing capabilities are typically highly dependent on their surface [45]. Consequently, raising the high specific surface area of CuO nanoparticles has been the aim of this study.

## CHAPTER -2

### NANOMATERIALS AND SYNTHESIS PROCESS

#### 2.1 NANOMATERIALS

"Nanomaterials" are materials with a minimum of one nanoscale dimension (usually between 1 and 100 nanometres) (length, width, or height). In comparison to their bulk counterparts, materials frequently display distinctive and unexpected features at this scale. Based on their composition, structure, and behaviour, nanomaterials can be divided into a number of groups. Based on dimensionality nanomaterial can be classified as,

1. **Nanoparticles:** Particles that fall into the nanometre range are known as nanoparticles. Materials include metals, metal oxides, and polymers that can be used to create them. Drug delivery, imaging, and catalysis are just a few of the many uses for nanoparticles.
2. **Nanotubes:** Having diameters in the nanoscale range, nanotubes are hollow tubes. Known for their remarkable mechanical, thermal, and electrical qualities are carbon nanotubes. Materials science, electronics, and even the medical domains find uses for them.
3. **Nanocomposites:** The materials known as nanocomposites combine the qualities of nanoparticles and nanofillers by incorporating them into a matrix material. The improved mechanical, thermal, or electrical properties of nanocomposites make them useful in the aerospace, automotive, and construction industries.
4. **Nanowires:** Having a diameter in the nanometer range, nanowires are incredibly tiny wires. Semiconductors, solar cells, sensors, and transistors all employ nanowires because of their special optical and electrical characteristics.
5. **Nanorods:** Nanorods are long, elongated objects with sizes that go into the nanoscale range. They find application in the domains of electronic devices, optics, and catalytic processes.
6. **Quantum Dots:** Man-made nanoscale crystals known as quantum dots (QDs) have special optical and electrical characteristics. When exposed to UV light, they may



transport electrons and release a variety of coloured lights. These synthetic semiconductor nanoparticles offer a plethora of possible uses, such as solar cells, composites, displays, illumination, fluorescent biological labelling, and medical imaging.

7. **Graphene:** Graphene is a carbon allotrope which consists of a single sheet of atoms organised in a lattice with a hexagonal shape nanostructure. Because the graphite allotrope of carbon contains a large number of double bonds, the term is formed from the word "graphite" and the suffix -ene. It has applications in energy storage, electronics, and materials research.

Nanomaterials has unique properties and a broad variety of applications that could totally revolutionize several industries. While much research is being done to better understand and mitigate these risks, concerns have been raised over potential impacts on the environment and public health.

## 2.2 SYNTHESIS APPROACH

Different strategies are used to synthesize nanomaterials, each with the aim of achieving particular characteristics and uses. Common methods for synthesizing nanomaterials include the following

1. **Top-Down approach:** By using this technique, the bulk is split up into smaller pieces, which are then further broken up into nanomaterials.

Integrated circuit manufacturing serves as an illustration of this methodology. Nanocrystalline structures are formed by the division of macrocrystalline structures.

2. **Bottom-Up approach:** Nanomaterials are created by assembling the tiniest units, or atoms. It is employed in the construction of fundamental materials, such as the assembly of atoms and molecules.

Sol-gel, hydrothermal, physical, and chemical vapor deposition are a few of the techniques of Bottom-Up approach.

### 2.2.1 SYNTHESIS METHODS FOR NANOMATERIAL SYNTHESIS

Nanoparticles can be created using different techniques, each having unique profits and drawbacks. The size, shape, intended qualities of the nanoparticles, and the intended use all influence the synthesis technique selection. The following are some typical methods for creating nanoparticles:

- 1. Electrochemical Method:** In order to produce nanoparticles, metal ions must be reduced at the electrode surface during the electrochemical synthesis process. The electrochemical production of silver nanoparticles is one instance of this.
- 2. Green Synthesis Method:** Nanoparticles are synthesized from natural sources such as plant extracts or microorganisms. For example, aloe vera plant extract can be utilized to make silver nanoparticles.
- 3. Co-precipitation Method:** consists of two or more ingredients that precipitate at the same time to form nanoparticles. For example, iron oxide nanoparticles can be produced by co-precipitating iron salts and a base.
- 4. Chemical Reduction Method:** This process reduces metal ions using reducing agents to create nanoparticles. As an illustration, gold nanoparticles can be created by reducing gold chloride with a reducing agent like sodium borohydride.
- 5. Sol-Gel Process:** Using the Sol-Gel Process, a fluid is transformed into a gel that is subsequently dried and burned to create nanoparticles. For example, the sol-gel method is frequently used for producing silica nanoparticles.
- 6. Hydrothermal/Solvothermal Process:** A high-temperature, high-pressure environment is used to create nanoparticles. Example: A hydrothermal approach can be used to create metal oxide nanoparticles.
- 7. Microemulsion:** Technique: When water, oil, and surfactant are combined, nanoparticles are created. Example: A microemulsion technique can be used to create copper nanoparticles.
- 8. Combustion Synthesis Method:** The burning of precursor materials produces nanoparticles. An example of this would be the synthesis of titanium dioxide nanoparticles through burning.

- 9. Template-Assisted Synthesis Method:** This method makes use of a template to produce nanoparticles, which are subsequently extracted from the template [48]. Example: the synthesis of mesoporous silica nanoparticles with the use of a template.
- 10. Photochemical Synthesis Technique:** Photochemical reactions are used to produce nanoparticles. Example: Photochemical techniques can be used to create cadmium sulphide nanoparticles.
- 11. Mechanical Milling:** Technique: Grinding large quantities of material by hand produces nanoparticles. For example, different materials can be turned into nanoparticles by using high-energy ball milling.
- 12. Gas-Phase Synthesis:** The process of gas-phase synthesis involves the formation of nanoparticles, usually through the vaporization of a precursor material. Example of this is the production of gas phase nanoparticles using laser ablation.

## CHAPTER -3

### HYDROTHERMAL SYNTHESIS OF CuO NANOPARTICLES

#### 3.1 HYDROTHERMAL METHOD

The hydrothermal technique uses water as a solvent in a closed system at a certain temperature and pressure to complete the reaction, simulating the formation of crystals during the mineralization process in sample [49]. Properties of water such as vapour pressure, density, viscosity, surface tension, and ionic product will all alter significantly in hydrothermal conditions [50]. It is clearly capable of lowering system reaction temperatures and producing highly crystalline products with small size distributions, excellent purity, and little aggregation [51]. As the reaction is in the closed system it is challenging to watch the material's growth process. The hydrothermal process also has a number of drawbacks, such as expensive equipment requirements, a lengthy reaction time, and significant energy consumption [52].

#### 3.2 SYNTHESIS PROCESS

##### 3.2.1 MATERIALS

Copper (II) nitrate trihydrate  $\text{Cu}(\text{NO}_3)_2 \cdot 3\text{H}_2\text{O}$ , Copper chloride anhydrous ( $\text{CuCl}_2$ ) and Urea were purchased from Sigma-Aldrich chemical company. The deionized water was used for various solution preparation having resistivity of  $18.2 \text{ M}\Omega \text{ cm}^{-1}$ . Ethanol was used for washing the precipitate.

##### 3.2.2 SAMPLE PREPARATION

A novel approach used for creating CuO nanostructures involved different precursors and different reaction temperature. Three different samples were prepared using two different precursors and two different synthesis temperature. Sample 1 abbreviated as S1 is synthesised by combining ( $\text{CuCl}_2$ ) with deionized water in a beaker to create a copper

(0.2 M) solution, which was then agitated with a magnetic stirrer until the solution turned light green. The solution above was combined with urea (0.2 M) while being continuously stirred. It was then put into the oven at 150 °C for 12 h in an autoclave. After cooling at room temperature, the resulting black precipitates was repeatedly cleaned with deionized water and ethanol to get rid of contaminants like surfactants. The precipitate was further dried for 6 h at 75 °C. Sample 2 abbreviated as S2 was synthesized keeping all the conditions same and by just changing the precursor from copper chloride anhydrous (CuCl<sub>2</sub>) to copper nitrate trihydrate Cu(NO<sub>3</sub>)<sub>2</sub>·3H<sub>2</sub>O. A 0.2 M solution of Cu(NO<sub>3</sub>)<sub>2</sub>·3H<sub>2</sub>O was prepared and rest process is kept same. For synthesis of sample 3 which is abbreviated as S3 was prepared by just increasing the reaction temperature of sample 2 from 150 °C to 180 °C. The three samples were compared and their properties were studied.

### 3.2.3 FILM DEPOSITION AND GAS SENSING MEASUREMENT

The doctor blade method was used to coat an alumina substrate with a thick layer of synthesised CuO nanoparticles. A binder called polyethylene glycol (PEG 200) has been utilised to coat the thick layer of generated nanoparticles on the substrate. The generated binder and CuO nanoparticle paste are applied to an alumina substrate using a doctor blade. After the coated film was sintered at 300 °C for an entire night, the applied silver paste was dried for 12 hours at 70 °C. Silver electrodes are made to measure electrical resistance. The film was then placed on top of an electric micro heater that was placed inside the 0.5 L chamber. The diluted volatile organic compounds (VOCs) were added to the bottom electric microheater at a concentration of 100 ppm using a micropipette. The vaporised VOCs moved upward as a result, interacting with the sensor material. Voltage is applied to the micro-heater to control the temperature of the sensor. Equation (1) was used to estimate the probe's sensitivity.

$$\text{Sensitivity } (S) = \frac{R_g}{R_a} \quad (1)$$

Where  $R_a$  is the initial resistance of CuO in presence of air before adsorption and  $R_g$  is the resistance after the adsorption of gas vapours.

### 3.2.4 SYNTHESIS STEPS

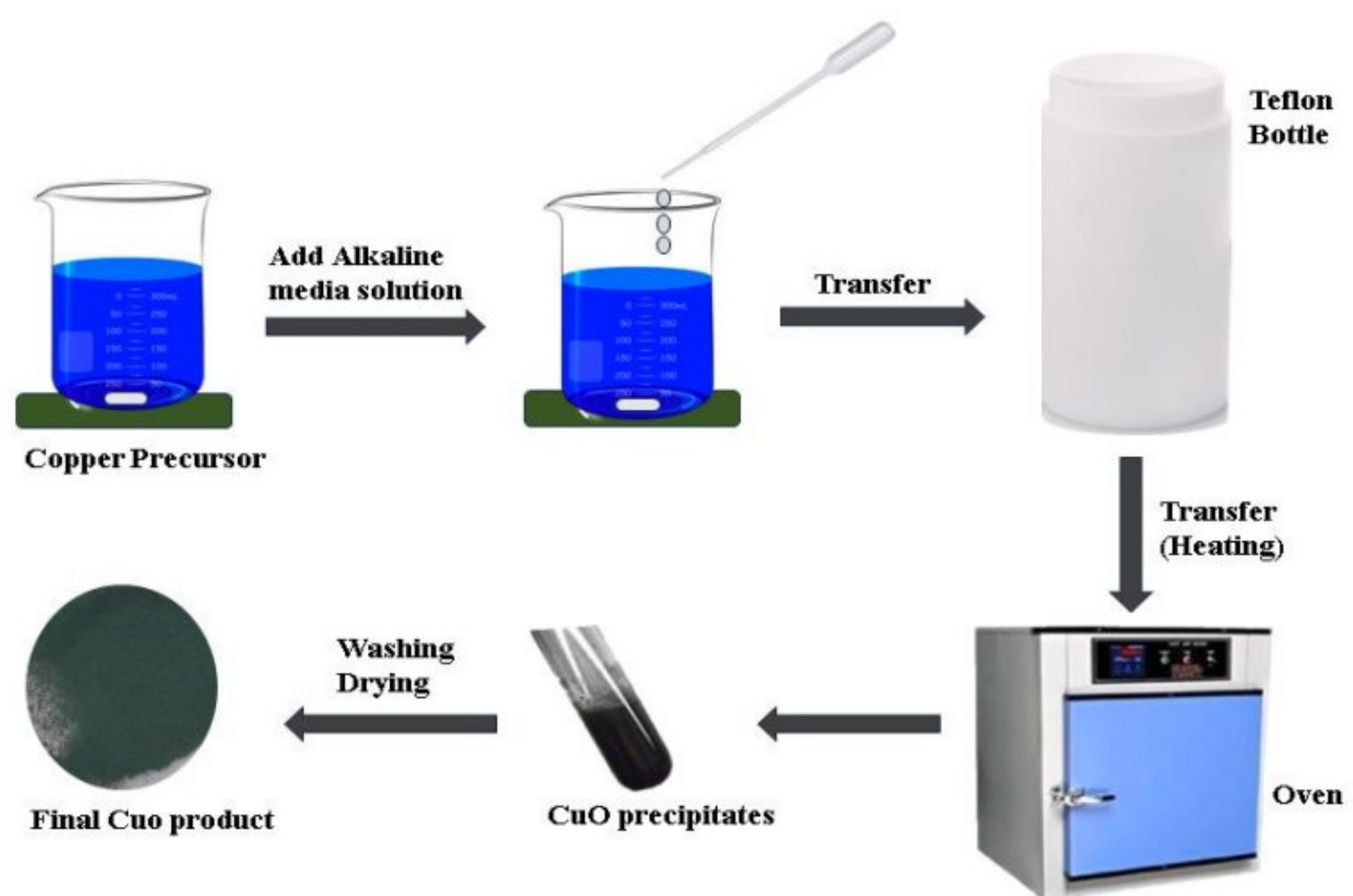


**Figure 3.1:** Schematic representation of synthesis process of CuO nanoparticles.

## CHAPTER -4

### RESULTS AND DISCUSSION

#### 4.1 CRYSTALLOGRAPHY ANALYSIS

Figures 4.1, 4.2, and 4.3 shows the XRD patterns of samples S1, S2, and S3, respectively. According to XRD examination, phase development of CuO nanoparticles was seen in all three produced samples. CuO is seen in the monoclinic phase in S1 and S2, along with some unreacted precursor impurities. XRD pattern analysis of sample S3 depicts the synthesized sample is pure without any impurity. Visible diffraction peaks of CuO indicate the monoclinic crystal structure of sample S3 from the standard JCPDS file No.: 00-045-0937, space group (S.G.): C2/c, S.G. No. 15. With  $\beta = 99.54^\circ$ , the unit cell parameters a, b, and c are seen as 0.458, 0.318, and 0.504 nm, respectively. Using Eq. (2), the parameters a, b, and c are estimated.

$$\frac{h^2}{a^2} + \frac{k^2}{b^2} + \frac{l^2}{c^2} = \frac{1}{d^2} \quad (2)$$

Here, h, k, and l are the miller indices and d is the interplanar spacing. Bragg's diffraction law, can be used to determine the value of d as given in Eq. (3)

$$2d\sin\theta = n\lambda \quad (3)$$

The position of the most intense peak can be seen at  $35.55^\circ$ . Using the value of FWHM (full width at half maxima) and the Debye-Scherrer equation [53] given as Eq. (4) is

$$t = \frac{0.9\lambda}{\beta\cos\theta} \quad (4)$$

here  $\theta$  = Bragg's diffraction angle,  $\lambda$  = x-ray wavelength, t = size of crystal, and  $\beta$  = FWHM (in radians). The calculated average crystallite size for sample S3 is 44 nm.

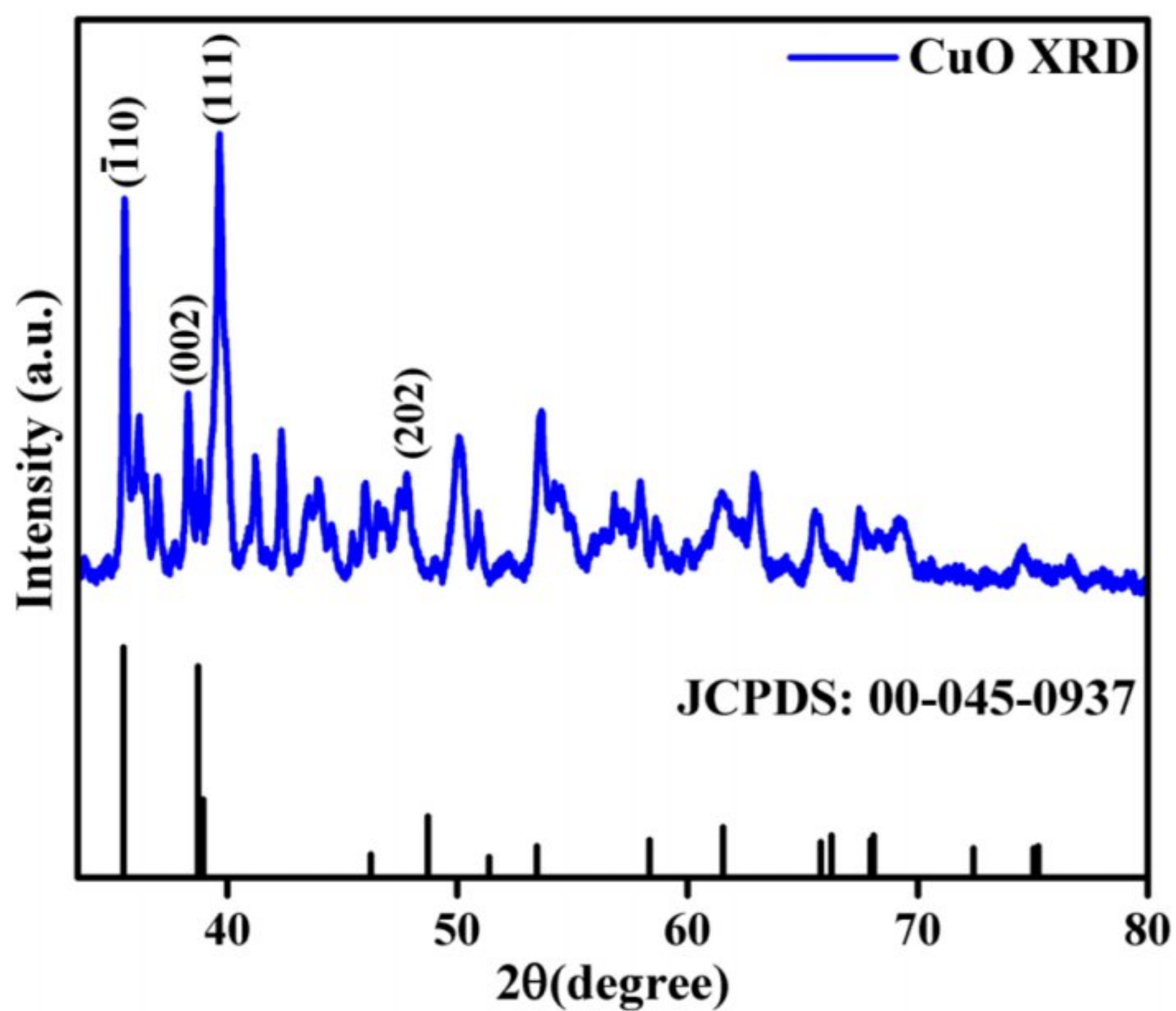


Figure 4.1: XRD pattern of sample S1 along with JCPDS file.

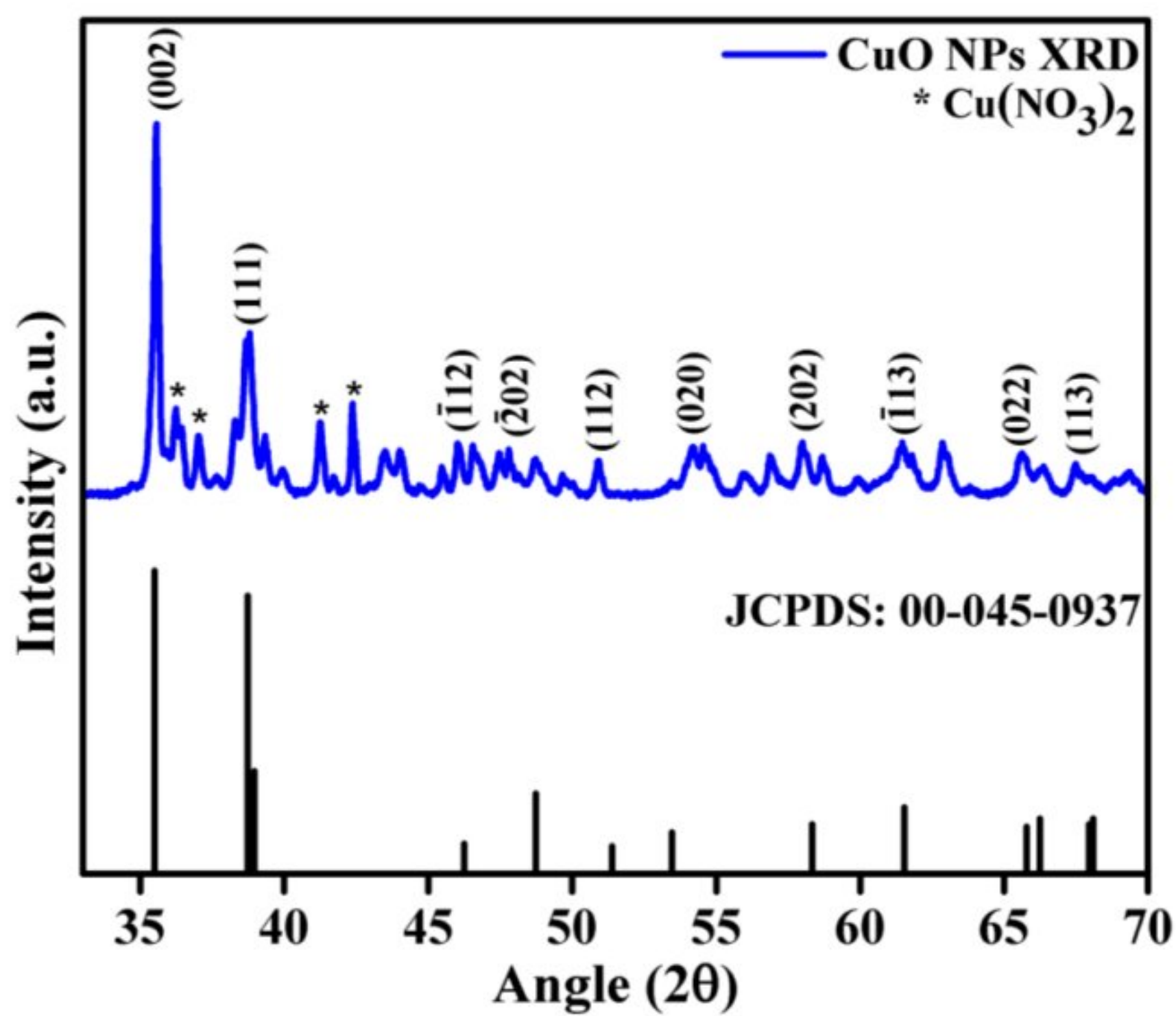


Figure 4.2: XRD pattern of sample S2 along with JCPDS file.



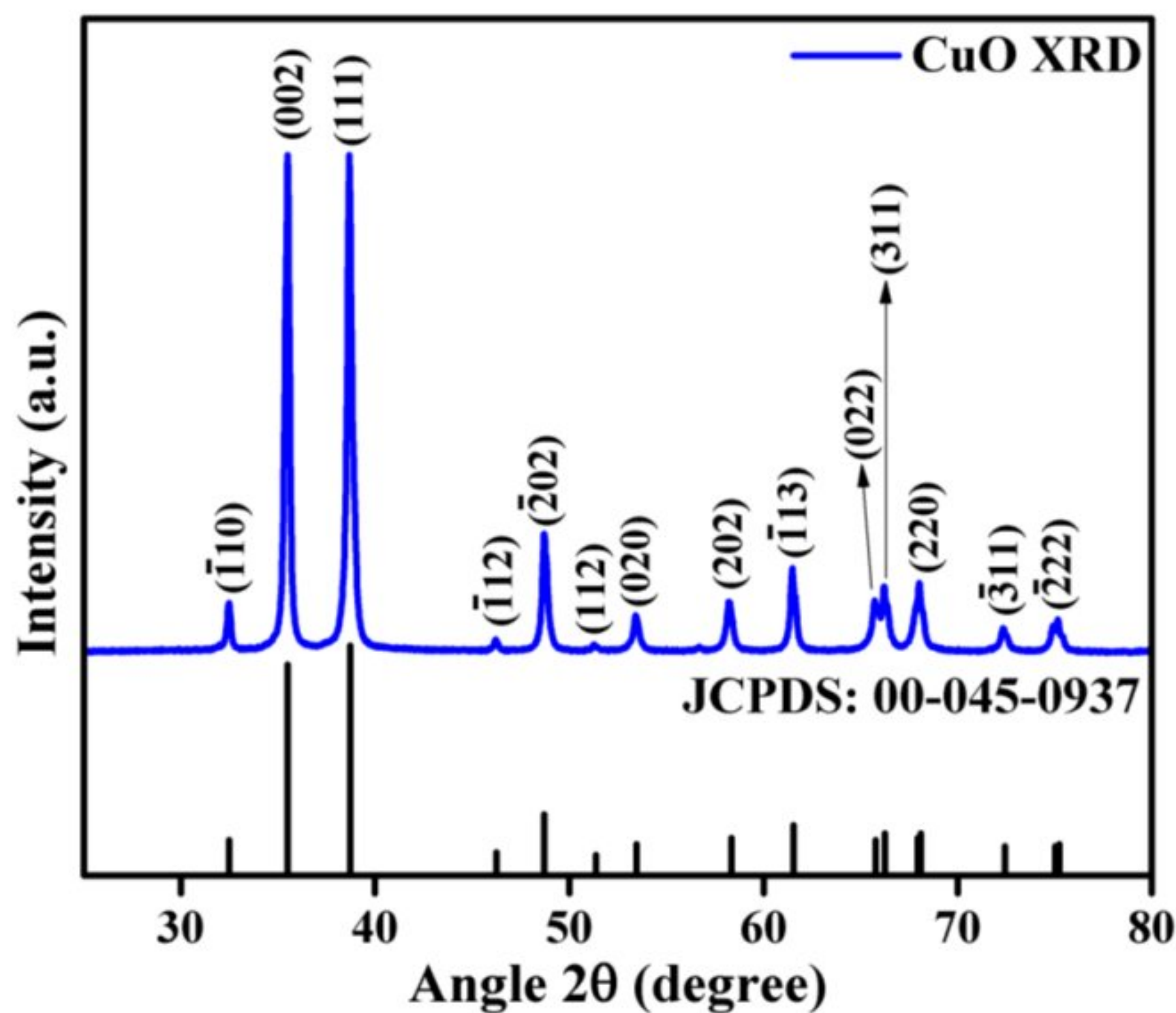
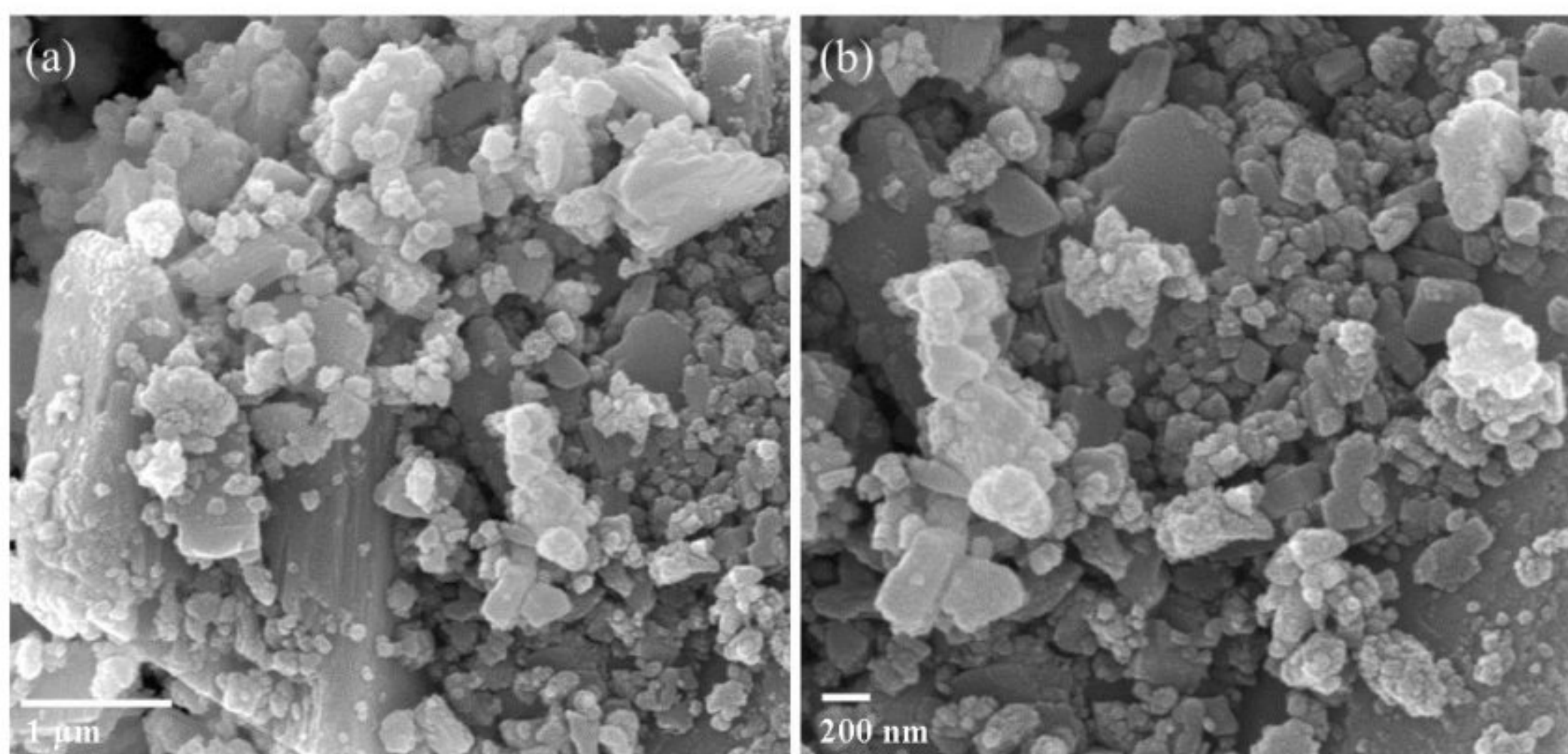


Figure 4.3: XRD pattern of sample S3 along with JCPDS file.

## 4.2 MORPHOLOGICAL ANALYSIS

Fe-sem analysis is done to examine the synthesised sample's morphology. Figures 4.4, 4.5, and 4.6 shows the Fe-sem images of samples S1, S2, and S3, respectively. Fe-sem images of particles at (a) low magnification and (b) high magnification are included in every figure. Figure 4.4 displayed for sample S1 illustrates the aggregation of particles. Particle formation is not uniform. Figure 4.5 illustrates the formation of particles with a cuboidal shape for sample S2. The arrangement of these cuboidal-shaped particles forms a ball like structure. Based on a high magnification picture, the average particle size for sample S2 is 135 nm. The Fe-sem pictures of S3, which demonstrate the creation of a petal-like structure of particles, are displayed in figure 4.7. These petals are arranged in a uniform pattern which forms a flower like pattern as an aggregate. The average particles size calculated for the sample S3 from high magnification image is 180 nm.



**Figure 4.4:** Fe-sem images of sample S1 synthesized using precursor Copper chloride

(a) 1 μm and (b) 200 nm.

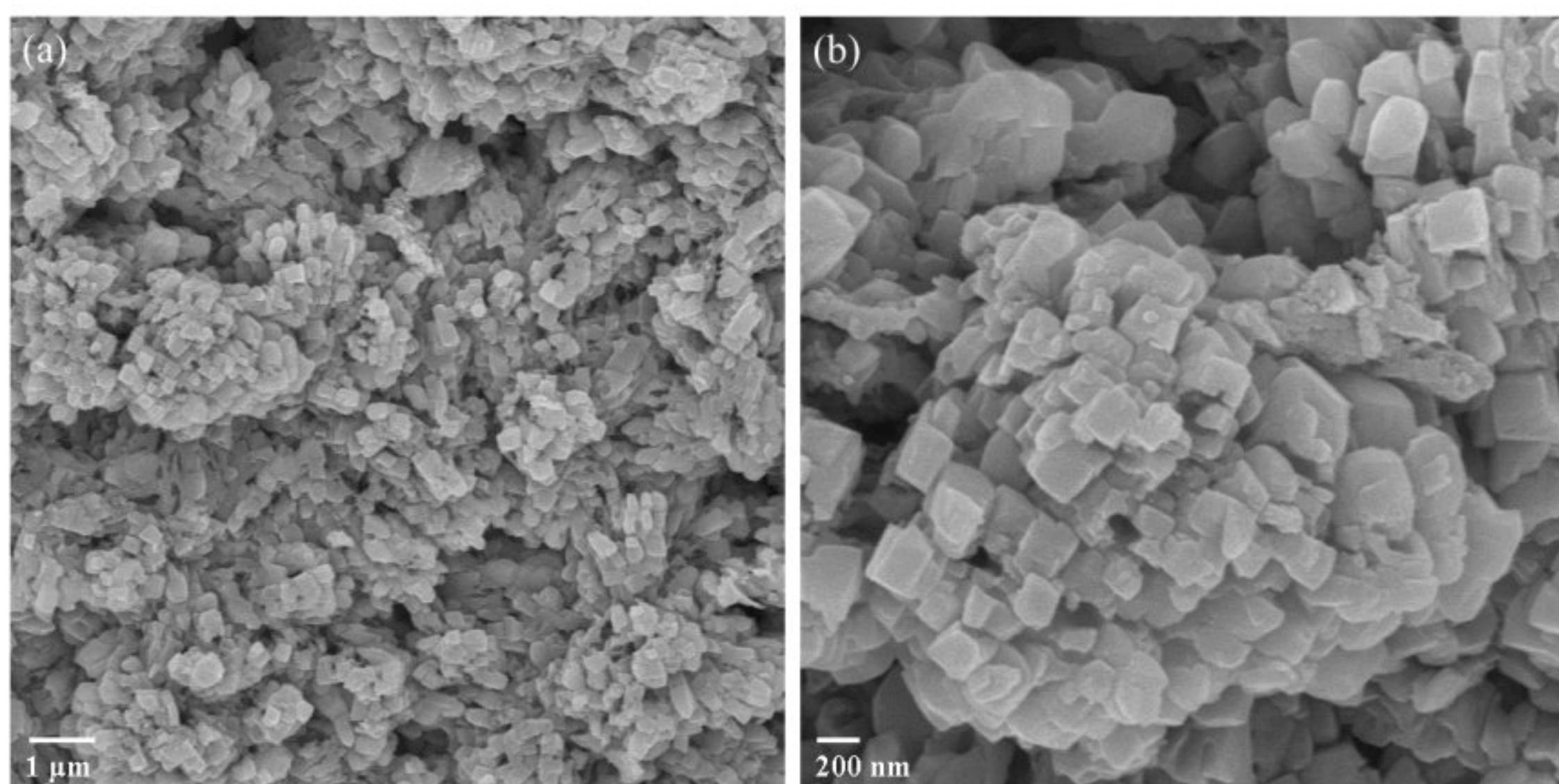


**Figure 4.5:** Fe-sem images of sample S2 synthesized using precursor Copper nitrate (a)

1 μm and (b) 200 nm.

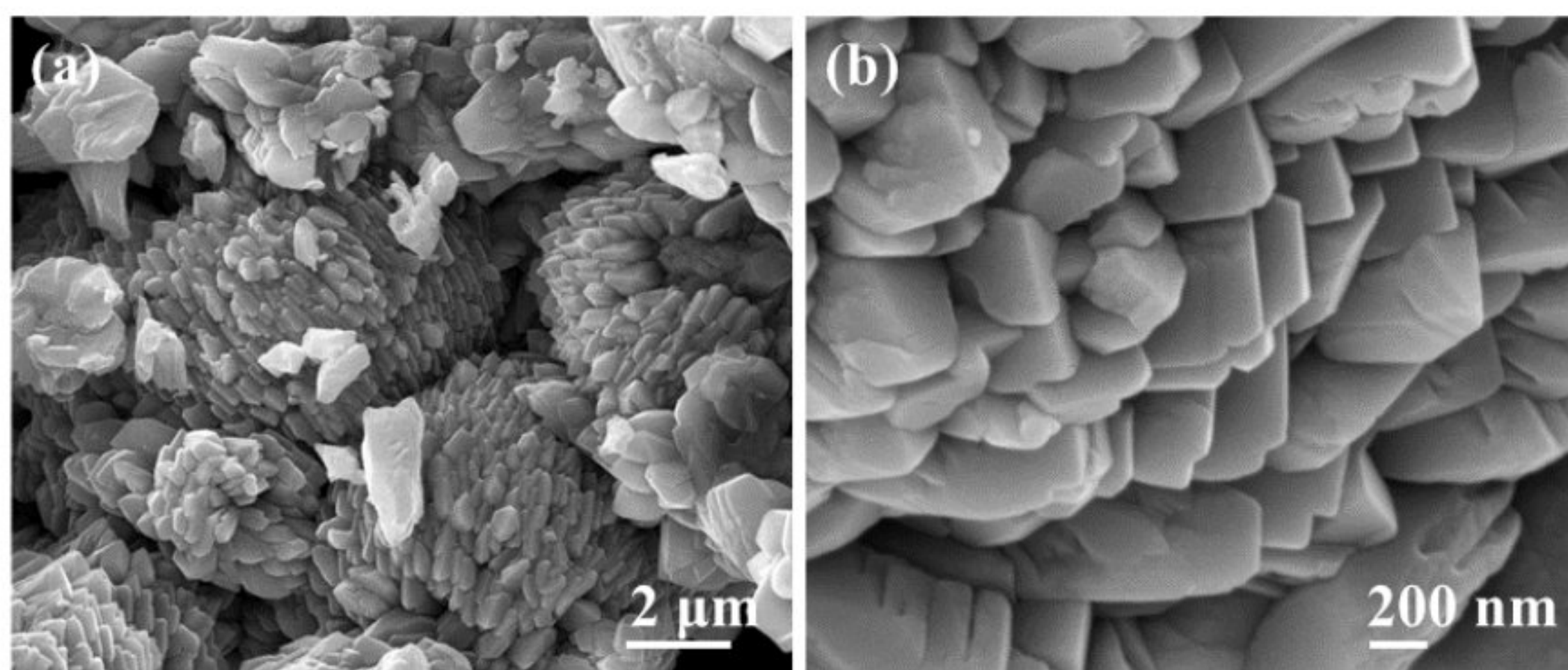


**Figure 4.6:** Fe-sem images of sample S3 synthesized using precursor Copper nitrate (a) 2 μm and (b) 200 nm.

### 4.3 EDX ANALYSIS

The elemental analysis of synthesized sample is done using (EDX) energy dispersive X-ray spectroscopy. Figure 4.7, 4.8, and 4.9 shows the EDX spectrum of sample S1, S2, S3 respectively. As seen from the figure 4.7 sample 1 contains major amount of Cu and oxygen. Table 4.1 shows the composition of all elements present in sample. According to this table the sample contains 56.42 % of Cu and 26.68 % of O as weight percentage. Weight percentage of 0.07 % of N and 1.05 % of Cl shows the presence of some unreacted precursors. Cu and O are present in an atomic percent of 22.74 % and 42.74 % respectively which suggest the formation of CuO. Cu and O are present in a stoichiometry ratio of 1:1.8 which shows the presence of excess oxygen.

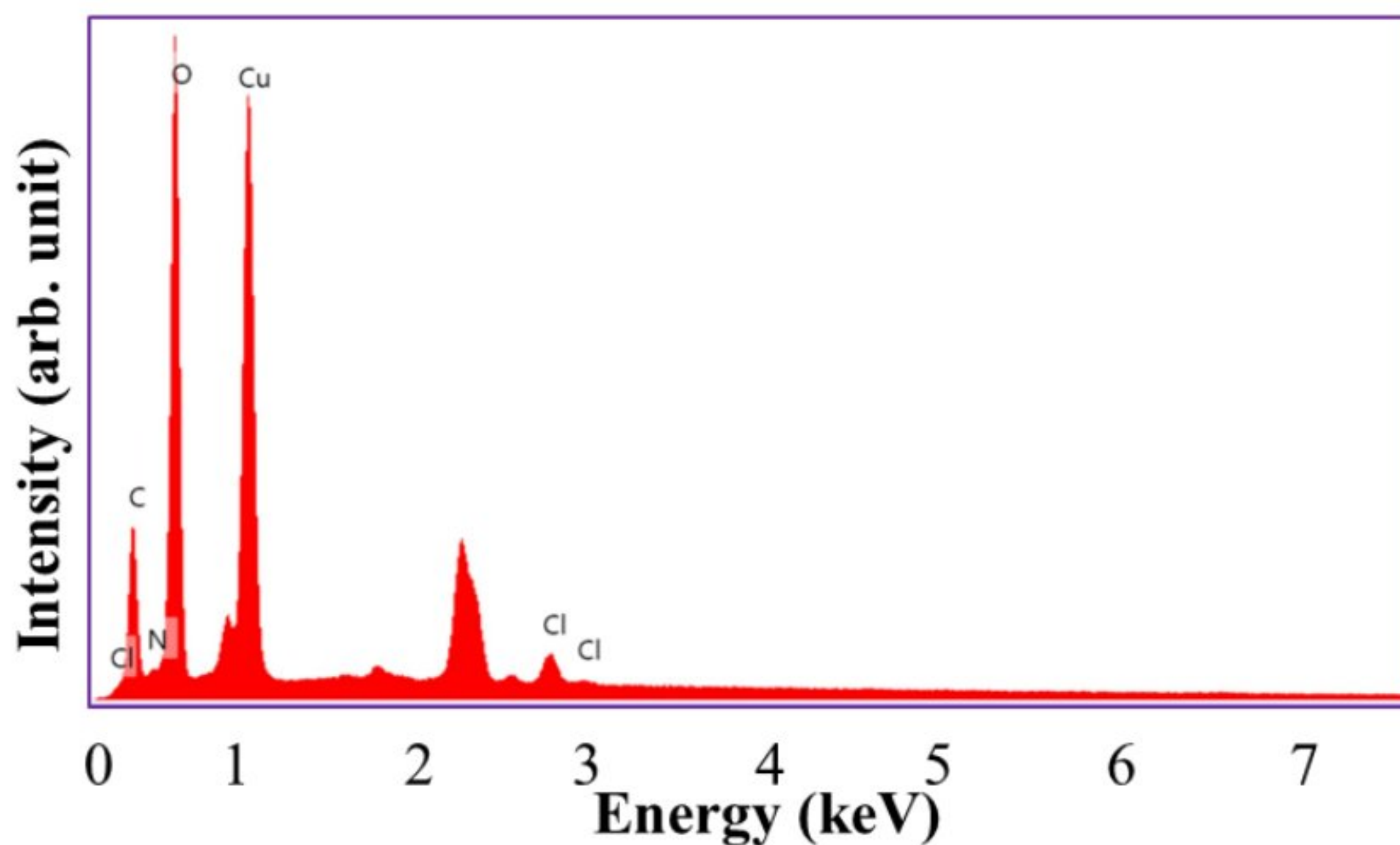


**Figure 4.7:** EDX spectra of sample S1 synthesized using copper chloride as precursor.

**Table 4.1:** Composition table showing atomic and weight percentage of elements in sample S1.

| Element | Weight % | Atomic % |
|---------|----------|----------|
| Cu      | 56.42    | 22.74    |
| O       | 26.68    | 42.72    |
| N       | 0.07     | 0.13     |
| Cl      | 1.05     | 0.76     |

As seen from the figure 4.8 sample 2 also contains major amount of Cu and oxygen. Table 4.2 shows the composition of all elements present in sample. According to this table the sample contains 79.67 % of Cu and 12.50 % of O as weight percentage. Weight percentage of 0.17 % of N shows the presence of some unreacted precursors. Cu and O are present in an atomic percent of 46.70 % and 29.11 % respectively which suggest the

formation of CuO. Cu and O are present in a stoichiometry ratio of 1.6:1 which shows the presence of some extra copper because of unreacted copper nitrate.

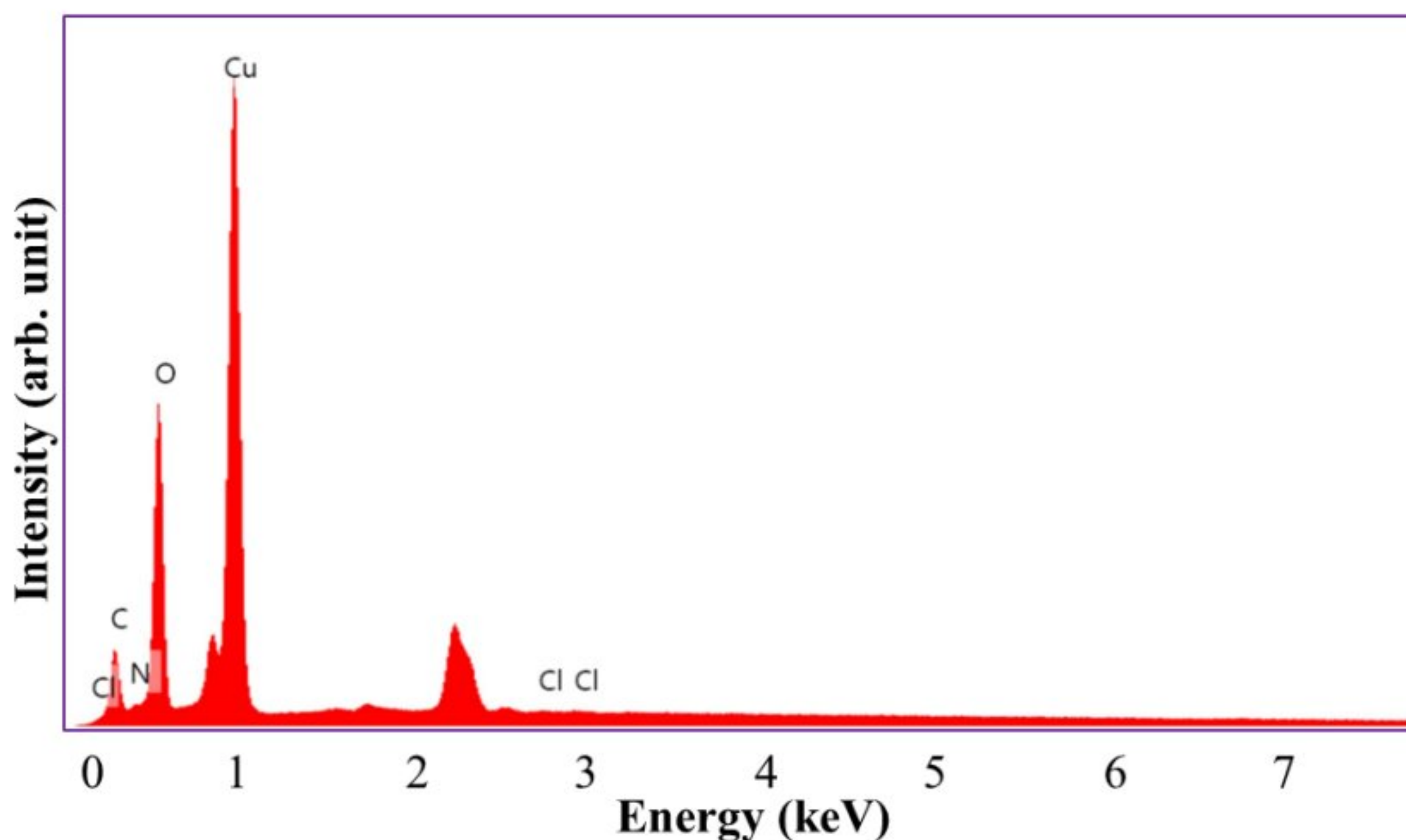


**Figure 4.8:** EDX spectra of sample S2 synthesized using copper nitrate as precursor.

**Table 4.2:** Composition table showing atomic and weight percentage of elements in sample S2.

| Element | Weight % | Atomic % |
|---------|----------|----------|
| Cu      | 79.67    | 46.70    |
| O       | 12.50    | 29.11    |
| N       | 0.17     | 0.44     |
| Cl      | 0.00     | 0.00     |

As seen from the figure 4.9 sample 3 contains only of Cu and oxygen. Table 4.3 shows the composition of Cu and O present in sample. According to this table the sample contains 82 % of Cu and 18 % of O as weight percentage. Cu and O are present in an

atomic percent of 53.4 % and 46.6 % respectively which suggest the formation of CuO. Cu and O are present in a stoichiometry ratio of 1.1:1 which suggest the formation of pure CuO.

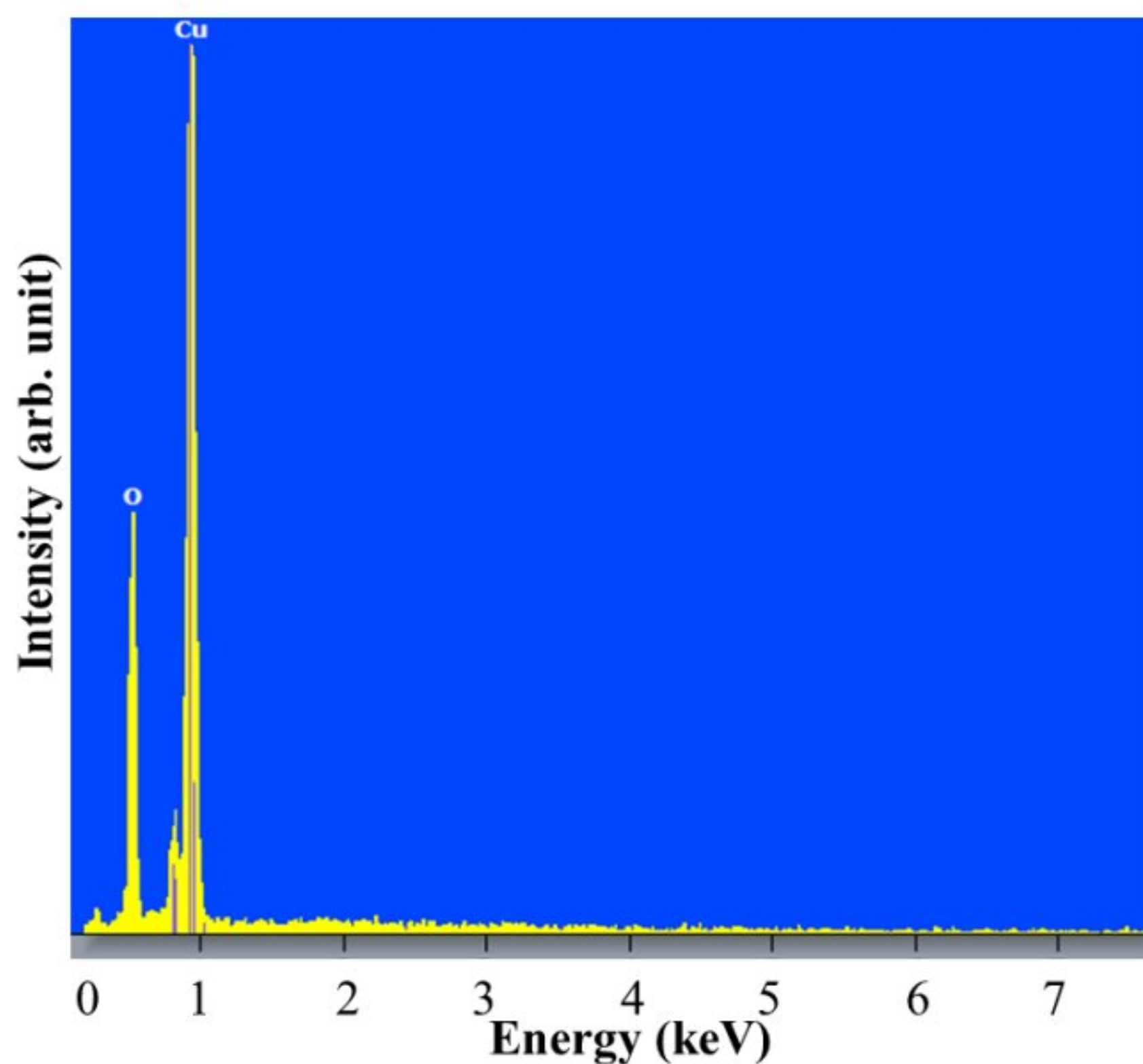


**Figure 4.9:** EDX spectra of sample S3 synthesized using copper nitrate as precursor.

**Table 4.3:** Composition table showing atomic and weight percentage of elements in sample S3.

| Element | Weight % | Atomic % |
|---------|----------|----------|
| Cu      | 82       | 53.4     |
| O       | 18       | 46.6     |

#### 4.4 FTIR ANALYSIS

To identify the various functional groups, present in the sample, an effective method for examining the molecular interactions and bonding characteristics of nanoscale materials is the FTIR technique. By monitoring the spectrum fingerprints obtained from the FTIR analysis, we can gather significant information on the functional groups present on the surface of the CuO NPs, clarifying their stabilization mechanism and structural stability. The identification of organic compounds, surfactants, or biomolecules that have been engaged in the synthesis process is made possible by FTIR analysis, which contributes to our understanding of the hydrothermal synthesis route. Functional groups involved in the synthesis of CuO NPs are studied using FTIR analysis of copper oxide nanoparticles obtained from the sample S2. The most likely functional group included in the sample can be identified using FT-IR analysis. Figure 4.10 displays the CuO nanoparticle's FT-IR spectrum.

In CuO nanoparticle's FT-IR spectrum analysis using  $\text{Cu}(\text{NO}_3)_2 \cdot 3\text{H}_2\text{O}$  as a precursor the Cu-O stretching vibrations of CuO nanoparticles can be seen from peaks at 746, 570 and  $520 \text{ cm}^{-1}$  along different faces of monoclinic structure. The band maxima at  $3398 \text{ cm}^{-1}$  and  $3310 \text{ cm}^{-1}$  are indicative of adsorbed water molecules and are OH stretching vibration and HOH bending modes [54,55] respectively. The transmittance band at 1042, 846 and  $815 \text{ cm}^{-1}$  are connected with Cu-(OH) and C-O stretching vibrations of alcohol, and phenolic-based compounds are denoted by peaks at 1491 and  $1376 \text{ cm}^{-1}$  [56].

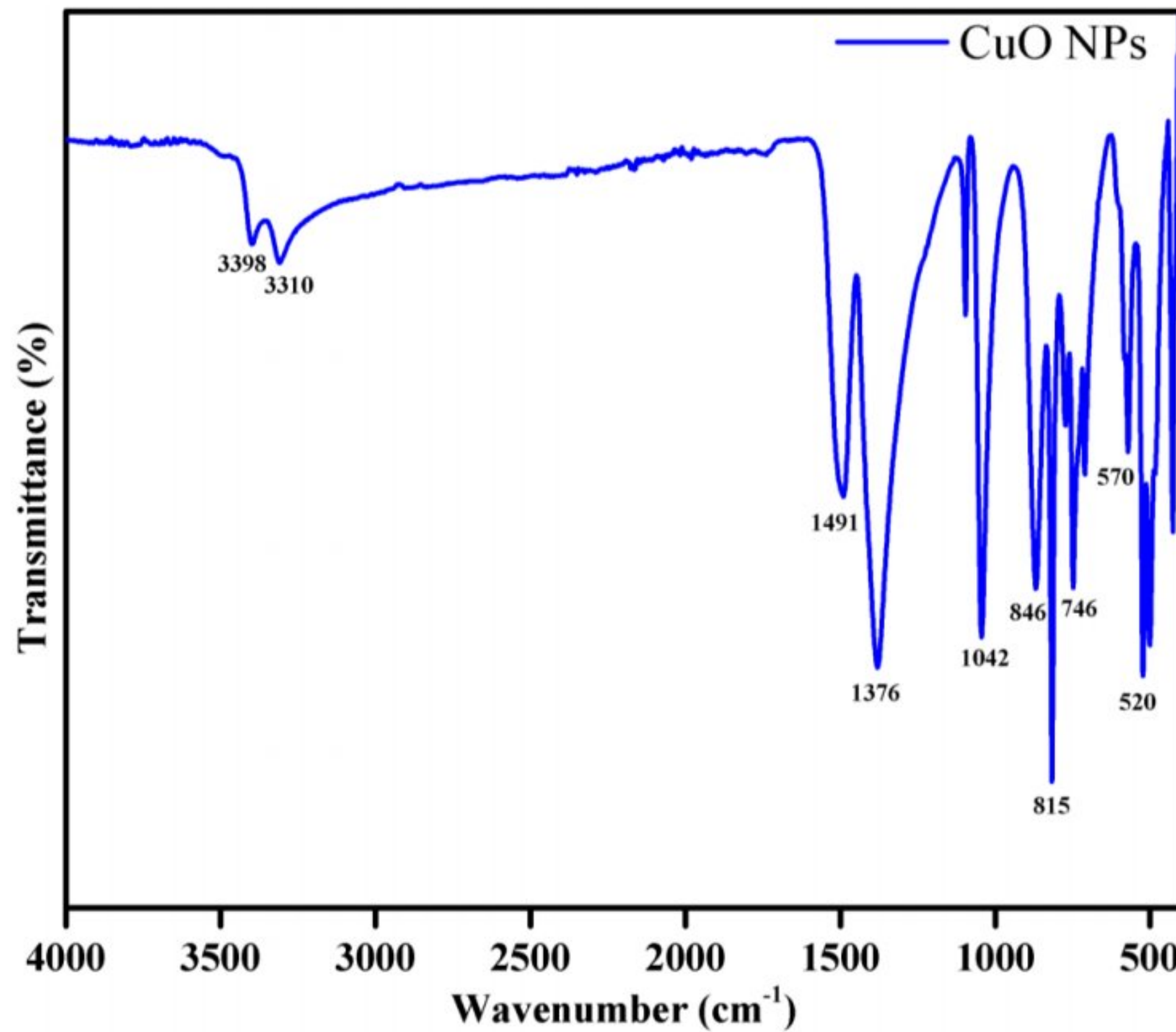


**Figure 4.10:** FTIR spectrum of Sample S2 synthesized using copper nitrate as precursor.

#### 4.5 UV-VISIBLE ANALYSIS

Spectroscopy study of sample S2 is done using UV-vis spectroscopy. The observed absorbance plot for the given sample is shown in figure 4.11. Acc. To the given data CuO nanoparticle's wide absorption band located about 292 nm. CuO nanoparticles with good transmittance were produced at a high temperature. Figure 4.12 shows CuO nanoparticle's indirect bandgap that is 3.4 eV which is consistent with values that have been previously published. Using the Tauc relation [57], one may ascertain the optical transition involved in the as-synthesized nanoparticles based on the dependency of  $\alpha$  on  $h\nu$ .

$$\alpha h\nu = \beta(h\nu - E_g)^n \quad (5)$$



Where  $n$  is a number, which is taken to be 0.5, 2 for direct and indirect transitions, respectively and  $\beta$  is constant.

It was discovered that the estimated bandgap for the particular temperature was found to be 3.4 eV. It was found that CuO nanoparticles synthesized at 150 °C had a bandgap energy that was similar to light energy in IR spectrum and could absorb more photons than copper oxide nanoparticles synthesized at other temperatures [58]. Therefore, it was assumed that CuO nanoparticles synthesized at 150 °C temperature would be a good fit for optoelectronics applications.

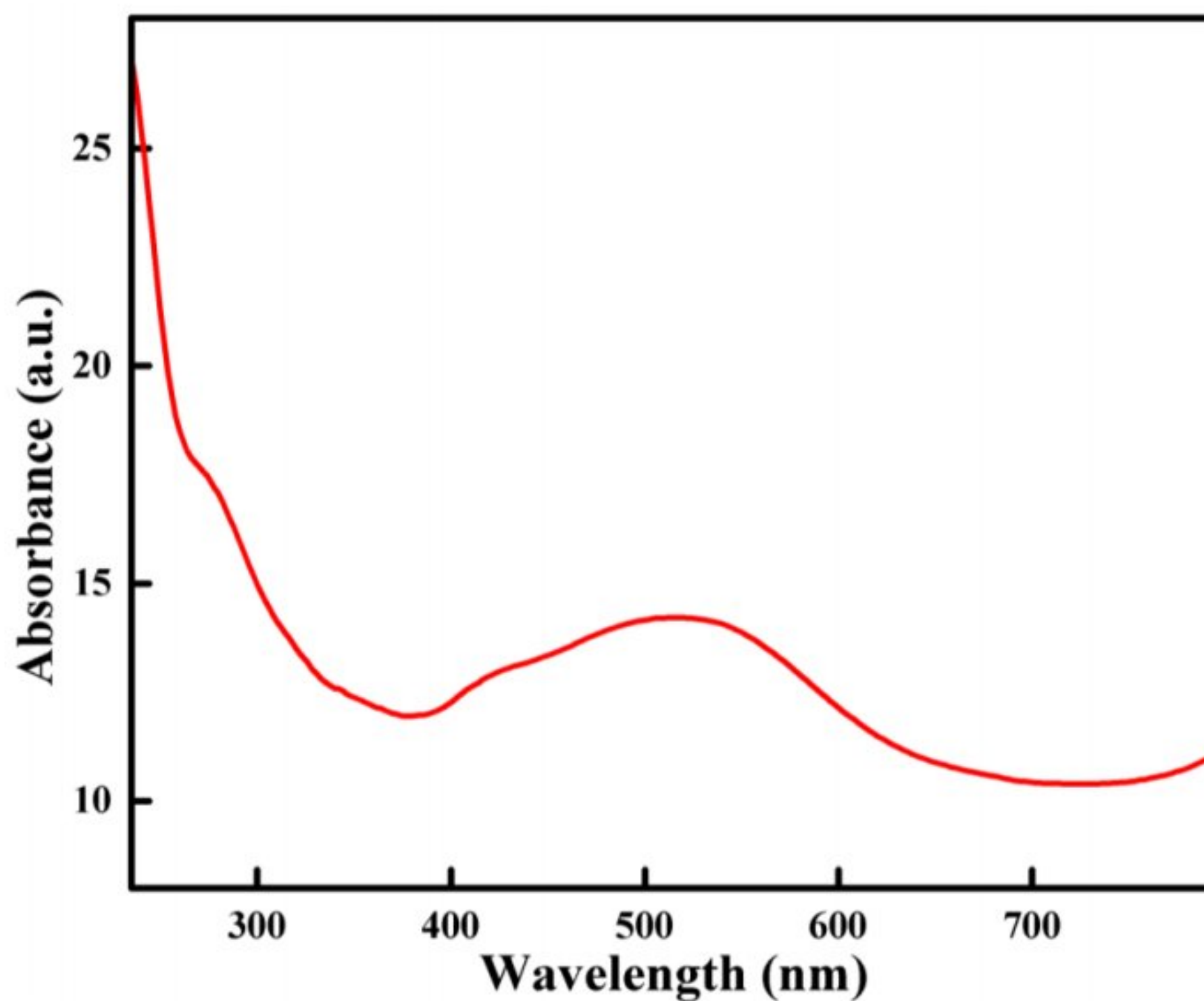


**Figure 4.11:** Absorption spectra of CuO synthesized at 150 °C using copper nitrate as precursor i.e. sample S2.

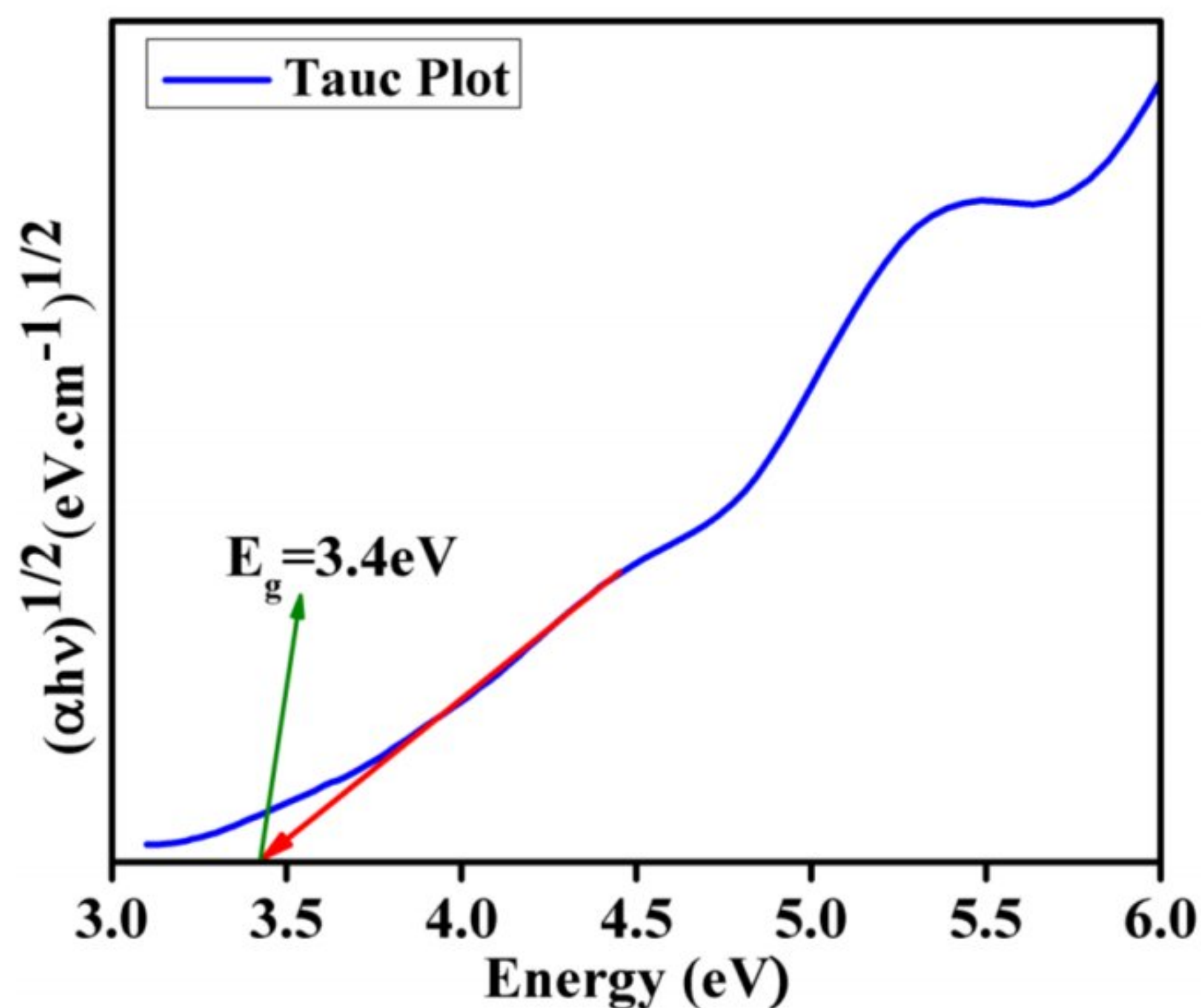


**Figure 4.12:** Tauc's plot for indirect bandgap of synthesized CuO nanoparticles sample S2.

#### 4.6 PHOTOLUMINESCENCE ANALYSIS

The photoluminescence (PL) analysis is performed for the sample S2. The photoluminescence (PL) spectrum of synthesised CuO nanoparticles with an excitation wavelength of 320 nm is shown in figure 4.12. At 417 nm, a unique PL band is found. The wide PL may be associated with defects and vacancies generated by non-stoichiometric CuO. The oxide material's emission wavelength is assumed to be significantly influenced by the particles' size, shape, and excitation wavelength [59]. The near band edge emission or exciton emissions can be seen at 417 nm in the PL spectrum [60,61]. The presence of Cu vacancies in CuO causes non-stoichiometry [62].

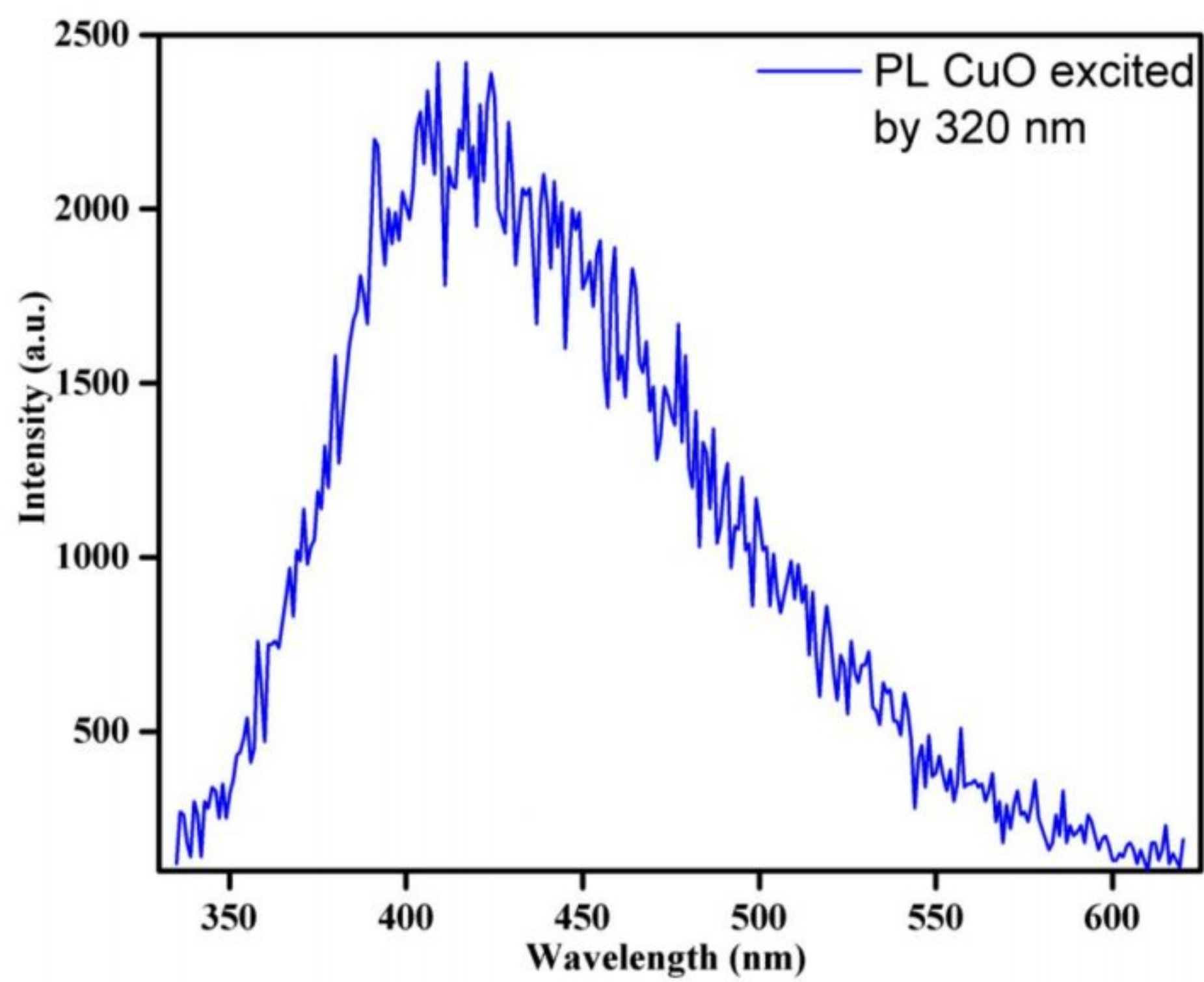


**Figure 4.13:** Emission spectra of CuO nanoparticles synthesized using copper nitrate as precursor at 150 °C.

## CHAPTER -5

### APPLICATIONS AS ACETONE GAS SENSOR

Acetone is a colourless liquid with a melting point of 94 °C, boiling temperature of 56.5 °C, density of 0.788 g/cm<sup>3</sup> and a distinct smell [63]. It is frequently used in labs and industries to dissolve plastic, purify paraffin, and dehydrate tissues. Inhaling acetone can cause irritation to the nose, throat, and eyes, which is harmful to one's health. It can also cause headache, nausea, dizziness, and sleepiness at high doses [63]. Thus, it is necessary to keep an eye on the acetone concentration. Acetone concentration measurement is aided by CuO nanoparticles. CuO particles have a high surface-to-volume ratio that makes it possible for gas molecules to adsorb on their surface, changing the electrical properties of the particles in remarkable ways. The CuO particle sensing mechanism originates from the interaction between the pre-adsorbed oxygen on CuO and the acetone gas. O<sup>-</sup> may be produced by pre-adsorbed oxygen interacting with CuO by charge exchange. A reaction happens between CuO and pre-adsorbed oxygen when it is subjected to acetone, which has a reductive tendency. The reactions between the pre-adsorbed O<sup>-</sup> and the acetone molecules neutralise the majority carrier in p-type CuO and liberate free electrons. This alteration results in fewer holes in CuO, which increases sensor resistance. The quantity of oxygen adsorbed on the CuO surface rises as the acetone concentration falls. As a result, the sensor resistance decreases and approaches the initial stable condition of CuO. Acetone concentration changed from 100 ppm to 50 ppm. The temperature used for the gas sensing experiment was 300 °C. Figure 7 displays the generated resistance vs time graph. The graph displays the acetone responses for six distinct acetone sensing cycles. The drop in acetone concentration is the cause of the peak maxima's declination. It is evident from the graph that the sample has a very low reaction and recovery time. Based on a concentration of 100 ppm, the sensor displays a reaction time of around 10 seconds and a recovery time of roughly 30 seconds. It is evident from the sensitivity formula  $c$  that the sample exhibits good sensitivity. As it can be seen from the plot, the resistance increases from 15K Ohmic resistance to about 500K Ohmic resistance on exposure to acetone. The value of sensitivity now can be calculated from Equations 1 as

$$\text{Sensitivity } (S) = \frac{500K}{15K} = 33.33 \quad (6)$$

Thus, a sensitivity of 33.33 is observed which shows that CuO is a good volatile gas sensor for gases like acetone.

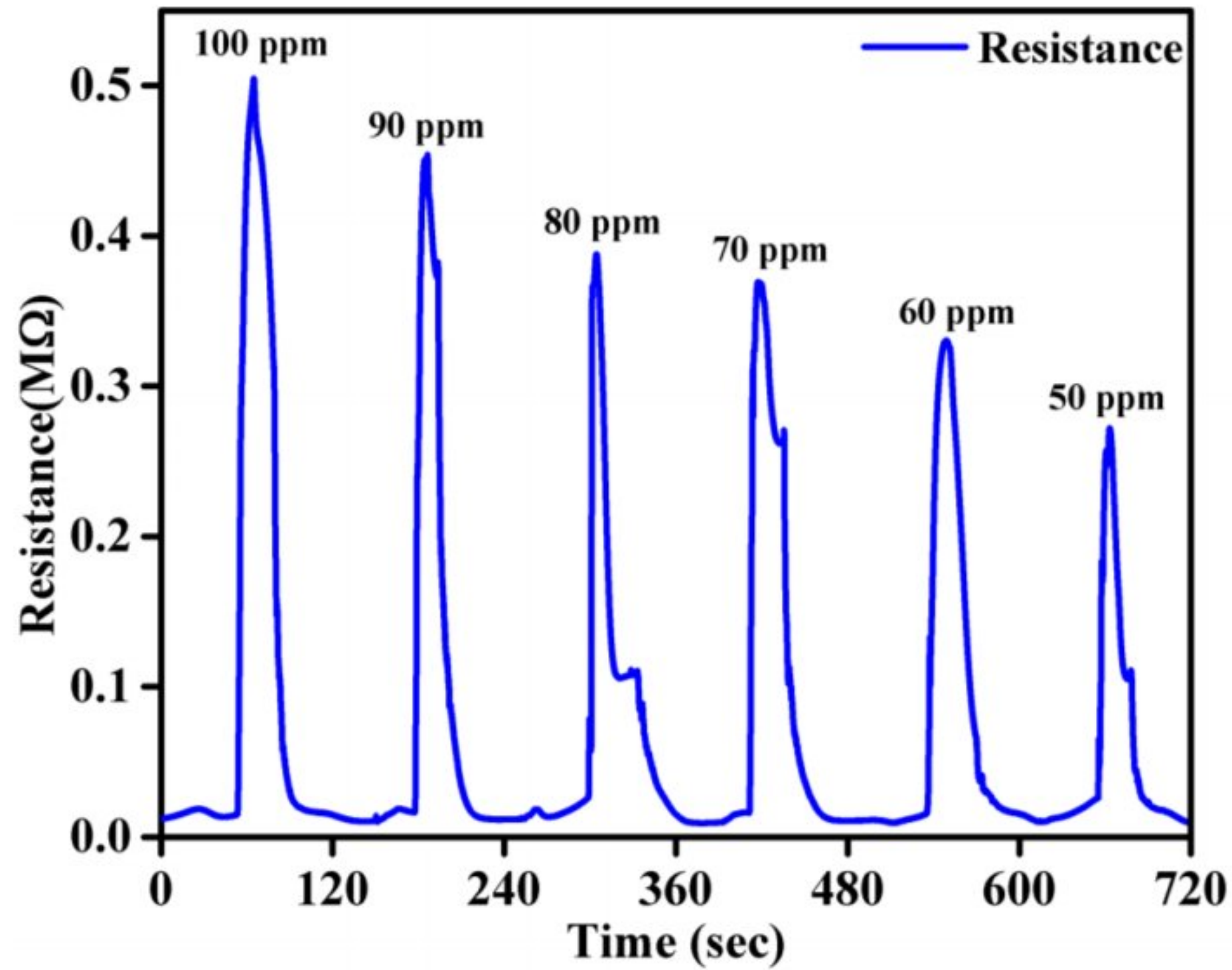


**Figure 5.1:** Variation of resistance (Ohm) with time for different cycles. Response recovery plot of CuO as acetone gas sensor at 300 °C.

## CHAPTER -6

### CONCLUSION

In the present work, three different samples of CuO nanoparticles have been successfully synthesized using different precursors and different reaction temperatures without using any surfactant via a cost-effective hydrothermal method. Various characterizations are performed to validate the successful synthesis of CuO nanoparticles which shows that the sample synthesized at 180 °C using copper nitrate trihydrate as precursors are formed without any impurity. The formation of cuboidal and petal shaped nanoparticles is confirmed by FESEM analysis. Phase and lattice parameters analysis is also done using the XRD method. Crystallite size is calculated for the most intense peak, which is found to be 44 nm for S2. EDX analysis is used to check the composition of Cu and O and FTIR is performed to detect the presence of functional groups in synthesized sample. EDX confirmed formation of CuO nanoparticles in stoichiometry with some impurities of copper nitrate in S2. FTIR confirmed the presence of Cu-O bonds in the sample. Photoluminescence analysis is also performed which is used to confirm the presence of defects in the sample. Further, gas sensing properties of CuO nanoparticles were studied for S2, sample showed a sensitivity of 33.33 for acetone gas which depicts CuO as a low cost and highly efficient sensor for sensing volatile gases like acetone.

## Bibliography:

- [1] Aishajiang R, Liu Z, Wang T, Zhou L, Yu D. "Recent Advances in Cancer Therapeutic CopperBased Nanomaterials for Antitumor Therapy". *Molecules*. 2023 Mar 1;28(5):2303. doi: 10.3390/molecules28052303. PMID: 36903549; PMCID: PMC10005215.
- [2] N. Dasgupta, S. Ranjan, and C. Ramalingam, "Applications of nanotechnology in agriculture and water quality management," *Environ. Chem. Lett.*, vol. 15, no. 4, pp. 591–605, 2017, doi: 10.1007/s10311-017-0648-9.
- [3] P. Ghosh, G. Han, M. De, C. K. Kim, and V. M. Rotello, "Gold nanoparticles in delivery applications", *Adv. Drug Deliv. Rev.*, vol. 60, no. 11, pp. 1307–1315, 2008, doi: 10.1016/j.addr.2008.03.016.
- [4] Ian Sullivan, Brandon Zoellner, and Paul A. Maggard, "Copper(I)-Based p-Type Oxides for Photoelectrochemical and Photovoltaic Solar Energy Conversion", *Chemistry of Materials* 2016 28 (17), 5999-6016, DOI: 10.1021/acs.chemmater.6b00926.
- [5] Jain, S., Mehata, M.S. "Medicinal Plant Leaf Extract and Pure Flavonoid Mediated Green Synthesis of Silver Nanoparticles and their Enhanced Antibacterial Property". *Sci Rep* 7, 15867 (2017). <https://doi.org/10.1038/s41598-017-15724-8>.
- [6] Saleem, Shahroz, Jabbar, Abdullah Hasan, Jameel, Muhammad Hasnain, Rehman, Azka, Kareem, Zahraa Hashim, Abbas, Ali Hashim, Ghaffar, Zunaira, Razzaq, Saba Abdul, Pashameah, Rami Adel, Alzahrani, Eman, Ng, Eng-Poh and Sapuan, Salit Mohd. "Enhancement in structural, morphological, and optical properties of copper oxide for optoelectronic device applications". *Nanotechnology Reviews*, vol. 11, no. 1, 2022, pp. 2827-2838. <https://doi.org/10.1515/ntrev-2022-0473>.
- [6] Siddiqi, K.S., Husen, A. "Current status of plant metabolite-based fabrication of copper/copper oxide nanoparticles and their applications: a review". *Biomater Res* 24, 11 (2020). <https://doi.org/10.1186/s40824-020-00188-1>.
- [7] Kolhatkar, Arati & Jamison, Andrew & Litvinov, Dmitri & Willson, Richard & Lee, T. (2013). "Tuning the Magnetic Properties of Nanoparticles. *International journal of molecular sciences*". 14. 15977-6009. 10.3390/ijms140815977.
- [8] A. Umer, S. Naveed, N. Ramzan, and M. S. Rafique, "Selection of a suitable method for the synthesis of copper nanoparticles". *Nano*, vol. 7, no. 5, 2012, doi: 10.1142/S1793292012300058.

- [9] Gao, X.P., Bao, J.L., Pan, G.L., Zhu, H.Y., Huang, P.X., Wu, F. and Song, D.Y. 2004, "Preparation and electrochemical performance of polycrystalline and single crystalline CuO nanorods as anode materials for Li-ion battery". *Journal of Physical Chemistry*, 108(2): 5547–5551.
- [10] Topnani, N. & Kushwaha, Surendra & Athar, Taimur. (2010). "Wet Synthesis of Copper Oxide Nanopowder. *International Journal of Green Nanotechnology*". *Materials Science & Engineering*. 1. M67-M73. 10.1080/19430840903430220.
- [11] Kim, Y.S., Hwang, I.S. and Kim, S.J. 2008. "CuO nanowire gas sensors for air quality control in automotive cabin". *Journal of Sensors and Actuators*, 135(1): 298-303.
- [12] Bohr, R.H., Chun, S.Y., Dau, C.W., Tan, J.T. and Sung, J. 2009. "Field emission studies of amorphous carbon deposited on copper nanowires grown by cathodic arc plasma deposition". *Journal of Carbon Material*, 24: 97-101.
- [13] Jiatao Zhang, Junfeng Liu, Qing Peng, Xun Wang, and Yadong Li, "Nearly Monodisperse Cu<sub>2</sub>O and CuO Nanospheres: Preparation and Applications for Sensitive Gas Sensors". *Chemistry of Materials* 2006 18 (4), 867-871, DOI: 10.1021/cm052256f.
- [14] Jianliang Cao, Yan Wang, Tianyi Ma, Yuping Liu, Zhongyong Yuan\* . "Synthesis of porous hematite nanorods loaded with CuO nanocrystals as catalysts for CO oxidation [J]". *Journal of Energy Chemistry*, 2011, 20(6): 669-676.
- [15] Vijaya, K.R., Elgamiel, R., Diamant, Y. and Gedanken, A. 2011. "Sonochemical preparation and characterization of nanocrystalline copper oxide embedded in poly(vinyl alcohol) and its effect on crystal growth of copper oxide". *Journal of Langmuir*, 17: 1406.
- [16] A. Umer, S. Naveed, N. Ramzan, and M. S. Rafique, "Selection of a suitable method for the synthesis of copper nanoparticles". *Nano*, vol. 7, no. 5, 2012, doi: 10.1142/S1793292012300058.
- [17] Gungure, Abel & Jule, Leta & Kiran, R. & Tyagi, Drdeepak & Ruby, A.Usha & Seenivasan, Venkatesh & Ramaswamy, Krishnaraj. (2021),. *Advances in Materials Science and Engineering*. 2021. 1-6. 10.1155/2021/7443664.
- [18] Dar, Mushtaq & Qurashi, Ahsanulhaq & Sun-young, Kim & Sohn, Jung Min & Kim, W.B. & Shin, Hyung-Shik. (2009). "Versatile synthesis of rectangular shaped nanobat-like CuO nanostructures by hydrothermal method; structural properties and growth mechanism". *Applied Surface Science - APPL SURF SCI*. 255. 10.1016/j.apsusc.2009.02.002.



- [19] Dörner, L., Cancellieri, C., Rheingans, B. et al. "Cost-effective sol-gel synthesis of porous CuO nanoparticle aggregates with tunable specific surface area". *Sci Rep* 9, 11758 (2019). <https://doi.org/10.1038/s41598-019-48020-8>.
- [20] N. Silva, S. Ramírez, I. Díaz, A. Garcia, and N. Hassan, "Easy, quick, and reproducible sonochemical synthesis of CuO nanoparticles". *Materials (Basel)*, vol. 12, no. 5, pp. 1–13, 2019, doi: 10.3390/MA12050804.
- [21] V. Anand and V. C. Srivastava, "Zinc oxide nanoparticles synthesis by electrochemical method: Optimization of parameters for maximization of productivity and characterization". *J. Alloys Compd.*, vol. 636, pp. 288–292, 2015, doi: 10.1016/j.jallcom.2015.02.189.
- [22] Ismat Zerín Luna, Lutfun Naher Hilary, A. M. Sarwaruddin Chowdhury, M. A. Gafur, Nuruzzaman Khan, Ruhul A. Khan, "Preparation and Characterization of Copper Oxide Nanoparticles Synthesized via Chemical Precipitation Method". *Open Access Library Journal*, Vol.2 No.3, 2015.
- [23] B. R. Gangapuram, R. Bandi, M. Alle, R. Dadigala, G. M. Kotu, and V. Guttena, "Microwave assisted rapid green synthesis of gold nanoparticles using *Annona squamosa* L peel extract for the efficient catalytic reduction of organic pollutants". *J. Mol. Struct.*, vol. 1167, pp. 305–315, 2018, doi: 10.1016/j.molstruc.2018.05.004.
- [24] Aklilu Guale Bekru, Osman Ahmed Zelekew, Dinsefa Mensur Andoshe, Fedlu Kedir Sabir, and Rajalakshmanan Eswaramoorthy "Microwave assisted synthesis of CuO Nanoparticles using *Cordia Africana* Lam. Leaf Extract for 4-Nitrophenol Reduction. *Journal of Nanotechnology* Volume 2021, Article ID 5581621 <https://doi.org/10.1155/2021/5581621>
- [25] Ekinci A, Kutluay S, Şahin Ö, Baytar O. "Green synthesis of copper oxide and manganese oxide nanoparticles from watermelon seed shell extract for enhanced photocatalytic reduction of methyleneblue". *IntJ Phytoremediation*.2023;25(6): 789-798. doi:10.1080/15226514.2022.2109588
- [26] Stagon, S. and Huang, H. (2013), "Synthesis and applications of small metallic nanorods from solution and physical vapor deposition. *Nanotechnology Reviews*, Vol. 2 (Issue 3)", pp. 259-267. <https://doi.org/10.1515/ntrev-2013-0001>.
- [27] El-Eskandarany, M Sherif et al. "Mechanical Milling: A Superior Nanotechnological Tool for Fabrication of Nanocrystalline and Nanocomposite Materials." *Nanomaterials (Basel, Switzerland)* vol. 11,10 2484. 24 Sep. 2021, doi:10.3390/nano11102484
- [28] Ryland C. Forsythe, Connor P. Cox, Madeleine K. Wilsey, and Astrid M. Müller , "Pulsed Laser in Liquids Made Nanomaterials for Catalysis," *Chemical Reviews* 2021 121 (13), 7568-7637, DOI: 10.1021/acs.chemrev.0c01069.

- [29] S. S. Joshi, S. F. Patil, V. Iyer, and S. Mahumuni, "Radiation induced synthesis and characterization of copper nanoparticles," *Nanostructured Mater.*, vol. 10, no. 7, pp. 1135–1144, 1998, doi: 10.1016/S0965-9773(98)00153-6.
- [30] T. A. Kareem and A. A. Kaliani, "Glow discharge plasma electrolysis for nanoparticles synthesis", *Ionics (Kiel)*, vol. 18, no. 3, pp. 315–327, 2012, doi: 10.1007/s11581-011-0639-y
- [31] C. P. Devatha and A. K. Thalla, "Green Synthesis of Nanomaterials. Mangalore", India: Elsevier Ltd., 2018.
- [32] Srivastava, S., Kumar, M., Agrawal, A. and Kumar, D. 2013. "Synthesis and characterization of copper oxide nanoparticles", *Journal of Applied Physics*, 5(4): 61-65
- [33] Rejith S.G. and Krishnan, C. 2008. "Synthesis of Cadmium-doped copper oxide nanoparticles", *Advances in applied Science Research*, 4(2): 103-10
- [34] Shkhorukov, Y.P., Gizhevskii, B.A., Mostovshchikova, E.V., Yermakov, A.Y., Tugushev, S.N. and Kozlov, E.A. 2006. "Nanocrystalline copper oxide for selective solar energy absorbers", *Physics Letter*, 32(2): 132-135.
- [35] Sambandam, A., 2010. "Solar energy material". *Journal of Solar Cells*, 91: 843-845.
- [36] Choi, H.H., Park, J. and Singh, R.K. 2004, "Nanosized CuO encapsulated silica particles using an electrochemical deposition coating", *Electrochemical Solid-State Letter*, 7:10–12.
- [37] Rehman, S., Mumtaz, A. and Hasanain, S.K. 2008 Size effects on the magnetic and optical properties of CuO nanoparticles. *Journal of Nanopartles Research*, 13: 2497-2499
- [38] Poole, C.P., Datta, T., Farach, H.A., Rigney, M.M. and Sanders, C.R. 1998. Copper oxide. superconductors. *Journal of Wiley-Interscience*, 145-147
- [39] Jain, S., Mehata, M.S. "Medicinal Plant Leaf Extract and Pure Flavonoid Mediated Green Synthesis of Silver Nanoparticles and their Enhanced Antibacterial Property". *Sci Rep* 7, 15867 (2017). <https://doi.org/10.1038/s41598-017-15724-8>
- [40] Chang, M.H., Liu, H.S. and Tai, C.Y. 2011. Preparation of copper oxide nanoparticles and its application in nanofluid. *Journal of Powder Technology*, 2(3): 207-378
- [41] Sathiya, S.M. & Okram, Gunadhor & Jothi Rajan, Michael. (2017). "Structural, Optical And Electrical Properties Of Copper Oxide Nanoparticles Prepared Through Microwave Assistance". *Advanced Materials Proceedings*. 2. 371-377. 10.5185/amp.2017/605.

- [42] Li, G., Dimitrijevic, N.M., Chen, T., Rajhand, K.A. and Gray, A. 2008. Role of surface/Interfacial Cu<sup>2+</sup> Sites in the photocatalytic activity of coupled CuO/TiO<sub>2</sub> nanocomposite. *Journal Physical Chemistry*, 112:19040-19044
- [43] Dubal, D.P., Dhawale, D.S., Salunkhe, R.R., Jamdade, V.S. and Lokhande, C.D. 2010. Fabrication of copper oxide multilayer nanosheets for supercapacitor application. *Journal of Alloy Compound*, 492: 26-30.
- [44] Ahmed, S., Rasual, M.G., Brownb, R. and Hashib, M.A. 2010. Influence of parameters on the heterogeneous photocatalytic degradation of pesticides and phenolic contaminants in waste water. *Journal of Environmental Management*, 9: 311-330
- [45] Li, Yueming & Liang, Jing & Tao, Zhanliang & Chen, Jun. (2008). CuO particles and plates: Synthesis and gas-sensor application. *Materials Research Bulletin - MATER RES BULL.* 43. 23802385. 10.1016/j.materresbull.2007.07.045.
- [46] Joudeh, N., Linke, D. Nanoparticle classification, physicochemical properties, characterization, and applications: a comprehensive review for biologists. *J Nanobiotechnol* 20, 262 (2022). <https://doi.org/10.1186/s12951-022-01477-8>
- [47] Ovais, Muhammad & Raza, Abida & Naz, Shagufta & Islam, Nazar Ul & Khalil, Ali & Ali, Shaukat & Khan, Muhammad & Shinwari, Zabta. (2017). Current state and prospects of the phytosynthesized colloidal gold nanoparticles and their applications in cancer theranostics. *Applied Microbiology and Biotechnology*. 101. 10.1007/s00253-017-8250-4.
- [48] Synthesis and Characterization of Aligned ZnO Nanorods on Porous Aluminum Oxide Template, Jiansheng Jie, Guanzhong Wang, Qingtao Wang, Yiming Chen, Xinhai Han, Xiaoping Wang, and J. G. Hou, *The Journal of Physical Chemistry B* 2004 108 (32), 11976-11980, DOI: 10.1021/jp048974r
- [49] Bharti DB, Bharati AV. Synthesis of zno nanoparticles using a hydrothermal method and a study its optical activity: Characterisation of znonaoparticle and its optical activity. *Luminescence*. 32(3), 317-320 (2017).doi:10.1002/bio.3180.
- [50] Sharma N, Kumar S, Kumar J. Synthesis and structural properties of zno doped nanoparticles prepared by hydrothermal method. *Integrated Ferroelectrics*. 186(1), 115-119 (2018). doi:10.1080/10584587.2017.1370333.
- [51] Ramimoghadam D, Bin Hussein MZ, Taufiq-Yap YH. Hydrothermal synthesis of zinc oxide nanoparticles using rice as soft biotemplate. *Chemistry Central Journal*. 7(1), 1-10 (2013). doi:10.1186/1752-153X-7-136.
- [52] Aneesh PM, Vanaja KA, Jayaraj MK. Synthesis of zno nanoparticles by hydrothermal method. 6639(Conference Proceedings), 66390J-66390J-66399.

- [53] Bin Mobarak M, Hossain MS, Chowdhury F, Ahmed S (2022) *Arabian Journal of Chemistry* 15:104117. doi: 10.1016/J.ARABJC.2022.104117
- [54] Mohassel R, Soofivand F, BahrAluloom YJ, Imran MK, Shabani-Nooshabadi M, Salavati-Niasari M (2023) *Int J Hydrogen Energy* 48:10955–10967. doi: 10.1016/J.IJHYDENE.2022.12.167
- [55] Sreekanth M, Srivastava P, Ghosh S (2020) Highly enhanced field emission from copper oxide nanoparticle decorated vertically aligned carbon nanotubes: Role of interfacial electronic structure. *Appl Surf Sci* 508:145215. doi: 10.1016/J.APSUSC.2019.145215
- [56] Srinivasa Rao K, Vanaja T (2015) Influence of Transition Metal (Cu, Al) Ions Doping on Structural and Optical Properties of ZnO Nanopowders. *Mater Today Proc* 2:3743–3749. doi: 10.1016/J.MATPR.2015.07.163
- [57] Volanti, D. P., Keyson, D., Cavalcante, L. S., Simoes, A. J., Joya, M. R., Longo, E., Varela, J. A., Pizani, P.S., Souza, A. G., “Synthesis and characterization of CuO flower-nanostructure processing by a domestichydrothermal microwave”. *J. Alloys Comp.* 459, 537–542 (2008).
- [58] Jillani, S., Jelani, M., Hafeez, M., Hassan, N. U., Ahmad, S., “Synthesis, characterization and biological studies of copper oxide nanostructures”. *Mater. Res. Express* 5(4) 045006 (2018) DOI: 10.1088/2053-1591/aab864.
- [59] Velázquez Lozada E, Camacho González GM, Torchynska T (2015) Photoluminescence emission and structure diversity in ZnO:Ag nanorods. *J Phys Conf Ser* 582. doi: 10.1088/1742-6596/582/1/012031
- [60] Vidyasagar CC, Naik YA, Venkatesh TG, Viswanatha R (2011) Solid-state synthesis and effect of temperature on optical properties of Cu–ZnO, Cu–CdO and CuO nanoparticles. *Powder Technol* 214:337–343. doi: 10.1016/J.POWTEC.2011.08.025
- [61] Wan J, Shi L, Benson B, Bruzek MJ, Anthony JE, Sinko PJ, Prudhomme RK, Stone HA (2012) Microfluidic generation of droplets with a high loading of nanoparticles. *Langmuir* 28:13143–13148. doi: 10.1021/LA3025952
- [62] Wei J, Zhao L, Peng S, Shi J, Liu Z, Wen W (2008) Wettability of urea-doped TiO<sub>2</sub> nanoparticles and their high electrorheological effects. *J Solgel Sci Technol* 47:311–315. doi: 10.1007/S10971-008-1787-Z
- [63] Yang Z, Rong Q, Bao T, Jiao M, Mao L, Xue X, Wen W, Wu Z, Zhang X, Wang S (2022) Synthesis of dual-functional CuO nanotubes for high-efficiently photoelectrochemical and colorimetric sensing of H<sub>2</sub>O<sub>2</sub>. *Anal Chim Acta* 1199:339598. doi: 10.1016/J.ACA.2022.339598

# PLAGIARISM REPORT

Similarity Report

PAPER NAME

Thesis Ankita Dahiya (2K22MSCPHY04),  
Bharat Bhushan (2K22MSCPHY07).docx

AUTHOR

Bharat Bhushan

WORD COUNT

10491 Words

CHARACTER COUNT

59083 Characters

PAGE COUNT

60 Pages

FILE SIZE

2.5MB

SUBMISSION DATE

Jun 6, 2024 1:28 PM GMT+5:30

REPORT DATE

Jun 6, 2024 1:30 PM GMT+5:30

## ● 4% Overall Similarity

The combined total of all matches, including overlapping sources, for each database.

- 3% Internet database
- 2% Publications database
- Crossref database
- Crossref Posted Content database
- 2% Submitted Works database

## ● Excluded from Similarity Report

- Bibliographic material
- Quoted material
- Cited material
- Small Matches (Less than 10 words)

Ankita

Bharat Bhushan



Summary

● **4% Overall Similarity**

Top sources found in the following databases:

- 3% Internet database
- 2% Publications database
- Crossref database
- Crossref Posted Content database
- 2% Submitted Works database

TOP SOURCES

The sources with the highest number of matches within the submission. Overlapping sources will not be displayed.

|   |   |     |
|---|---|-----|
| 1 | <b>University of Leeds on 2014-04-30</b><br>Submitted works                                 | <1% |
| 2 | <b>Deshraj Meena, Bharti Singh, Abhishek Anand, Mukhtiyar Singh, M.C. B...</b><br>Crossref  | <1% |
| 3 | <b>Ekaphan Swatsitang, Attaphol Karaphun, Thanin Putjuso. "Influence of ...</b><br>Crossref | <1% |
| 4 | <b>iGroup on 2015-04-27</b><br>Submitted works  | <1% |
| 5 | <b>tandfonline.com</b><br>Internet  | <1% |
| 6 | <b>text-id.123dok.com</b><br>Internet   | <1% |
| 7 | <b>nature.com</b><br>Internet   | <1% |
| 8 | <b>dspace.dtu.ac.in:8080</b><br>Internet  | <1% |

[Sources overview](#)

Similarity Report

|    |  |     |
|----|--|-----|
| 9  | <b>ir.haramaya.edu.et</b><br>Internet  | <1% |
| 10 | <b>uzspace.unizulu.ac.za:8080</b><br>Internet  | <1% |
| 11 | <b>ijacskros.com</b><br>Internet   | <1% |
| 12 | <b>Savitribai Phule Pune University on 2017-10-26</b><br>Submitted works                       | <1% |
| 13 | <b>Mohamed, Reda M., Farid A. Harraz, and Ahmed Shawky. "CuO nanobel...</b><br>Crossref        | <1% |
| 14 | <b>Pratima Bhat, Naveen Kumar S. K, P. Nagaraju. "Synthesis and charact...</b><br>Crossref     | <1% |
| 15 | <b>docshare.tips</b><br>Internet   | <1% |
| 16 | <b>moam.info</b><br>Internet   | <1% |
| 17 | <b>unsworks.unsw.edu.au</b><br>Internet  | <1% |
| 18 | <b>Amardeep Bajwa, Harpreet Kaur, Sanjeev Kumar, Gurjinder Singh. "Stu...</b><br>Crossref      | <1% |
| 19 | <b>G. Magesh, G. Bhoopathi, A.P. Arun, E. Ranjith Kumar, Ch. Srinivas, S. S...</b><br>Crossref | <1% |
| 20 | <b>Youngmi Cho, Changwook Kim, Heesung Moon, Youngmin Choi, Sohee...</b><br>Crossref           | <1% |

Sources overview

Similarity Report


|    |   |     |
|----|---|-----|
| 21 | <b>erepository.uonbi.ac.ke</b><br>Internet  | <1% |
| 22 | <b>mail.qaemiau.ac.ir</b><br>Internet   | <1% |
| 23 | <b>pubs.rsc.org</b><br>Internet   | <1% |
| 24 | <b>Mahdieh Razaghianpour, Mohammad Reza Hantehzadeh, Amir Hossei...</b><br>Crossref | <1% |
| 25 | <b>Universiti Sains Malaysia on 2012-11-07</b><br>Submitted works                   | <1% |
| 26 | <b>link.springer.com</b><br>Internet  | <1% |





Sources overview




## CONFERENCE RECORD

### PROOF OF REGISTRATION

ICAMNOP-2023 - Payment  
Acknowledgement Inbox 

 ICAMNOP-2023 29/11/2023     
to me ^

From ICAMNOP-2023 • icamnop@dtu.ac.in  
To bharatbhushanphysics@gmail.com  
Date 29 Nov 2023, 03:28  
 Standard encryption (TLS).  
[See security details](#)

Dear Mr. Bharat Bhushan,  
**Your payment has been successfully received**  
ICAMNOP-2023.  
Thanks and Regards  
Prof. Vinod Singh

## CERTIFICATE OF PARTICIPATION



## PROOF OF ACCEPTANCE

----- Forwarded message -----

From: **EquinOCS** <[equinocs-admins@springernature.com](mailto:equinocs-admins@springernature.com)>

Date: Thu, May 30, 2024 at 9:08 PM

Subject: Accepted paper in the EquinOCS system

To: Mohan Singh Mehata <[msmehata@dtu.ac.in](mailto:msmehata@dtu.ac.in)>

This message has been sent by the EquinOCS system  
<https://equinocs.springernature.com/>

PLEASE DO NOT REPLY

=====

Dear Mohan Singh Mehata,

We are pleased to inform you that your paper

056: "Surfactant Free and Facile Synthesis of Cuboidal Shaped CuO Nanoparticles for Acetone Sensing"

has been accepted for

International Conference on Atomic, Molecular, Material, Nano, and Optical Physics with Applications (ICAMNOP-2023)

## SCOPUS INDEXING



International Conference on Atomic, Molecular, Material,  
Nano and Optical Physics with Applications  
(ICAMNOP-2023)



Organized by: Department of Applied Physics, Delhi Technological University Delhi-  
110042, India  
December 20<sup>th</sup>-22<sup>nd</sup>, 2023

HOME CONFERENCE COMMITTEE SPEAKERS PUBLICATION REGISTRATION ABSTRACTS ACCOMMODATION TOUR GALLERY CONTACT US

Login

### Publication

The papers will be published in the Scopus indexed Springer's Proceedings in Physics (<https://www.springer.com/series/361>) after peer review.

Proceedings of our last International conference CAMNP 2019 was also published in Scopus indexed Springer's Proceedings in Physics  
<https://link.springer.com/book/10.1007/978-981-16-7691-8>

**Surfactant Free and Facile Synthesis of Cuboidal Shaped CuO Nanoparticles for Acetone Sensing**

Bharat Bhushan<sup>1</sup>, Ankita Dahiya<sup>1</sup>, Vinay Kumar Yadav<sup>1</sup>, Gagan Sharma<sup>2</sup> and Mohan Singh Mehata<sup>1,\*</sup>

<sup>1</sup>Laser and Spectroscopy Lab, Department of Applied Physics Delhi Technological University, Delhi - 110042, Delhi, India

<sup>2</sup>Clean Energy Research Laboratory, Department of Applied Physics Delhi Technological University, Delhi - 110042, Delhi, India

\*Correspondence: [msmehata@gmail.com](mailto:msmehata@gmail.com)

**Abstract.**

In this work, the CuO nanoparticles were effectively synthesized by the conventional hydrothermal method. A strong base was used for the precipitation of nanoparticles resulting in no templating agent being needed for the process to occur. X-ray diffraction pattern confirms nanoparticles have a crystallite size of 44 nm with a monoclinic phase of CuO. Highly dense and uniformly distributed particles can be seen by FESEM images. Bond vibration frequencies were used to detect the presence of Cu-O bond in the sample using FTIR spectroscopy. Compositional analysis was done with EDX spectroscopy. The photoluminescence (PL) analysis was performed and a peak maximum was observed at 417 nm might be due to the presence of defect states. Sensitivity analysis of acetone

depicts CuO has a low response and recovery time and is highly sensitive to acetone gas. Thus, a low-cost and efficient volatile gas sensor with a sustainable approach is proposed.

**Keywords:** CuO, Nanostructures, Hydrothermal Synthesis.

## **1 Introduction**

The creation of one-dimensional (1D) nanostructured materials, such as nanorods [1], nanoribbons [2], nanowires [3], and nanotubes [4] is interesting because of their special chemical, electrical, and mechanical qualities as well as their prospective uses. These properties of inorganic materials excited researchers for the production of materials with particular shape, size, and crystallinity during the past few decades. A significant amount of research has been done to synthesize various nanomaterials, such as semiconductors and metals. Electrical, optical and chemical characteristics depend mainly on nanomaterial's sizes, shapes, crystal structure, and surface morphology [5]. Copper oxide is a metal oxide which is present in two phases. In cupric oxide (CuO) vacancies of copper can be detected using deep level transient spectroscopy (DLTS) [6], which tells that it is a p-type semiconductor and has a bandgap ranging from 1.2 eV to 1.8 eV. Copper oxide (CuO) has been acknowledged as an industrially significant material for a wide range of useful applications, including gas sensing [7], solar energy conversion [8], batteries [2], catalysis [3], magnetic storage [3], and field emission [9]. Hence, the synthesis and analysis of CuO nanostructures should be crucial from both a fundamental and practical viewpoint. Over the past two decades, a number of methods, including the hydrothermal technique [10], solid-state reaction process [11], sol-gel method [12], and chemical vapour deposition [13], etc. have been employed to synthesize CuO nanostructures. The hydrothermal process is one of the suggested procedures that may be thought to be the most promising because of its low temperatures and high-pressure conditions. Here, we

describe the hydrothermal synthesis of CuO nanoparticles in the presence of urea using a simple efficient and surfactant-free technique. The success of the production of CuO nanoparticles is then confirmed using various characterization techniques.

## **2 Experimental**

### **2.1 Materials used**

$\text{Cu}(\text{NO}_3)_2 \cdot 3\text{H}_2\text{O}$  (copper (II) nitrate trihydrate), and strong base urea are purchased from Sigma-Aldrich chemical company are used, polyethylene glycol (PEG200), alumina substrate, silver paste for making electrodes are used in film production. The deionized water is used for various solution preparations having a resistivity of 18.2 M $\Omega$  cm. Ethanol is used for washing the precipitate.

### **2.2 Sample preparation and characterization**

A novel approach used for the synthesis of CuO nanostructures involved mixing  $\text{Cu}(\text{NO}_3)_2 \cdot 3\text{H}_2\text{O}$  in deionized water to get a copper (0.2 M) solution, which was then agitated with a magnetic stirrer until the solution turned light blue. The solution above is then intermixed with urea (0.2 M) while being continuously stirred. A temperature of 160 °C is given to the sample for 10 h to complete the reaction process in an autoclave, and the sample is collected after cooling. The resulting black precipitate is washed 3 to 4 times. The precipitate is then dried at 75 °C for 6 h. Figure 1 shows the stepwise representation of CuO nanoparticle synthesis. The prepared sample is then characterized using various techniques such as XRD, FESEM, FTIR, EDX and photoluminescence spectroscopy to analyze its crystallographic, morphological, elemental and optical properties.

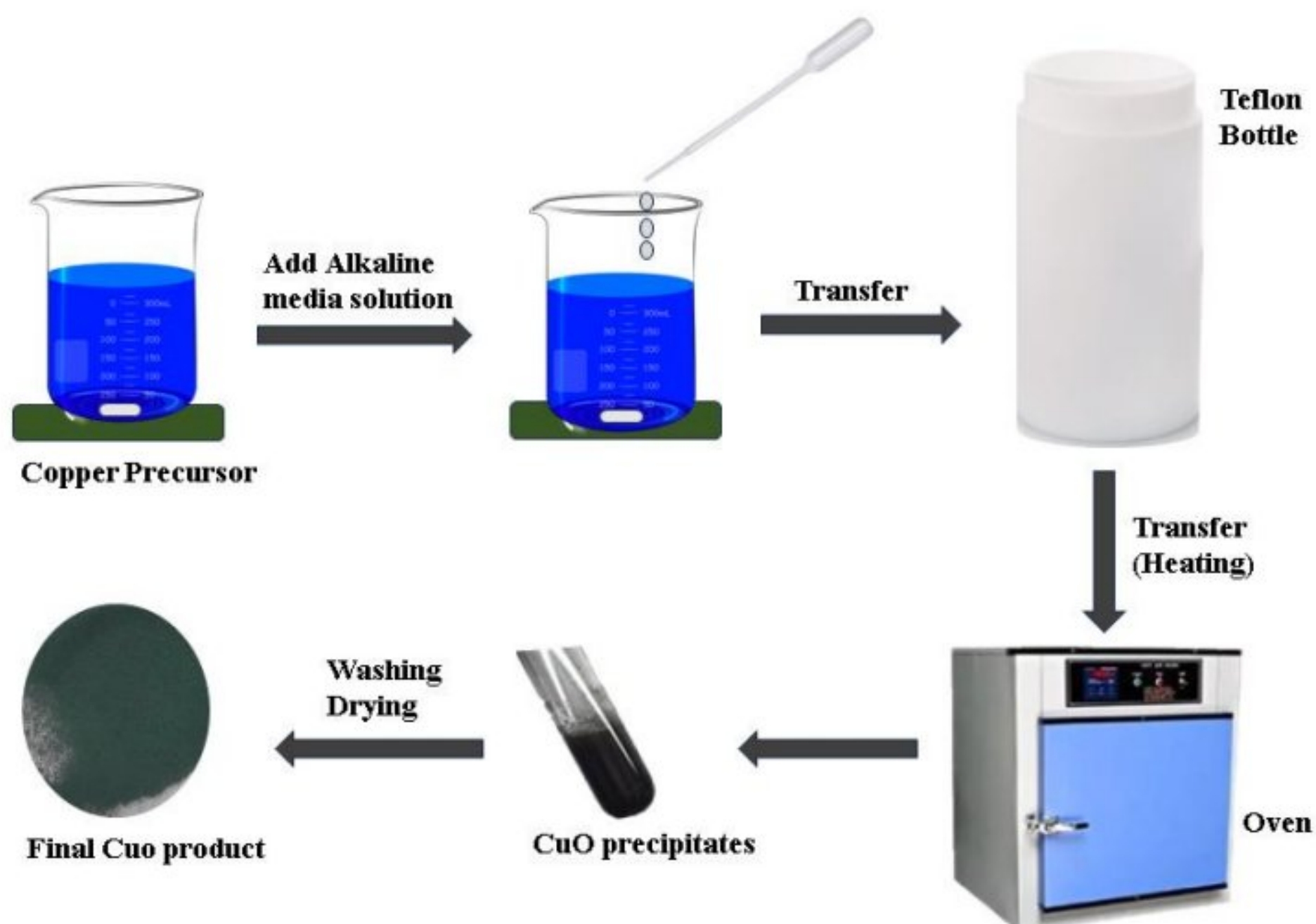


Figure 1. Stepwise representation of CuO nanoparticles synthesis.

### 2.3 Film deposition and gas sensing measurement

Using the doctor blade technique, a thick layer of synthesized CuO nanoparticles was created on an alumina substrate. To coat the thick layer of produced nanoparticles on the substrate, polyethylene glycol (PEG 200) has been used as a binder. Alumina substrate is coated with the produced binder and CuO nanoparticle paste using a doctor blade. In order to eliminate the binder and achieve good adhesion of nanoparticles with the substrate, the coated film was sintered at 300 °C overnight and then dried the applied silver paste for 12 hours at 70 °C. Now electrical resistance is measured from electrodes made of silver. The film was then set up on an electric micro heater that was positioned within the chamber of volume 0.5 L. A micropipette was used to introduce the diluted volatile organic compounds (VOCs) at a concentration of 100 ppm on the bottom electric microheater. This caused the vaporized VOCs to migrate upward and interact with the sensor material. The voltage delivered to the micro-heater was used to regulate the sensor's temperature.



The sensitivity of the probe was estimated with the following Eq. (1)

$$\text{Sensitivity } (S) = \frac{R_g}{R_a} \quad (1)$$

Where  $R_g$  is the resistance after the adsorption of gas vapours and  $R_a$  is the initial resistance of CuO in presence of air before adsorption.

### 3 Results and Discussion

#### 3.1 Crystallography Analysis

The XRD pattern of the synthesized sample is represented in Figure 2. The monoclinic crystal structure from the standard JCPDS file No.: 00-045-0937, space group (S.G.): C2/c, S.G. No.: 15 [14] is confirmed from visible diffraction peaks of CuO. The synthesized sample contains CuO with some minor impurities of unreacted copper nitrate that can be seen from JCPDS file no. 01-074-2372. The unit cell parameters  $a$ ,  $b$  and  $c$  can be seen as 0.458, 0.318 and 0.504 nm, respectively and  $\beta = 99.54^\circ$ . The parameters  $a$ ,  $b$  and  $c$  are estimated using Eq. (2).

$$\frac{h^2}{a^2} + \frac{k^2}{b^2} + \frac{l^2}{c^2} = \frac{1}{d^2} \quad (2)$$

here  $h$ ,  $k$ ,  $l$  are the miller indices of the planes from which X-ray is getting diffracted and  $d$  is the interplanar spacing. The value of  $d$  can be calculated using Bragg's diffraction law, Eq. (3)

$$2d\sin\theta = n\lambda \quad (3)$$

The position of the most intense peak can be seen at  $35.55^\circ$ . Using the value of FWHM (full width at half maxima) and the Debye-Scherrer equation [15] given as Eq. (4) is

$$t = \frac{0.9\lambda}{\beta\cos\theta} \quad (4)$$

here  $\lambda$  = wavelength of the x-ray used,  $\theta$  = Bragg's diffraction angle,  $t$  = size of the crystal, and  $\beta$  = FWHM (in radians). The calculated average crystallite size with the most intense peak is 44 nm.

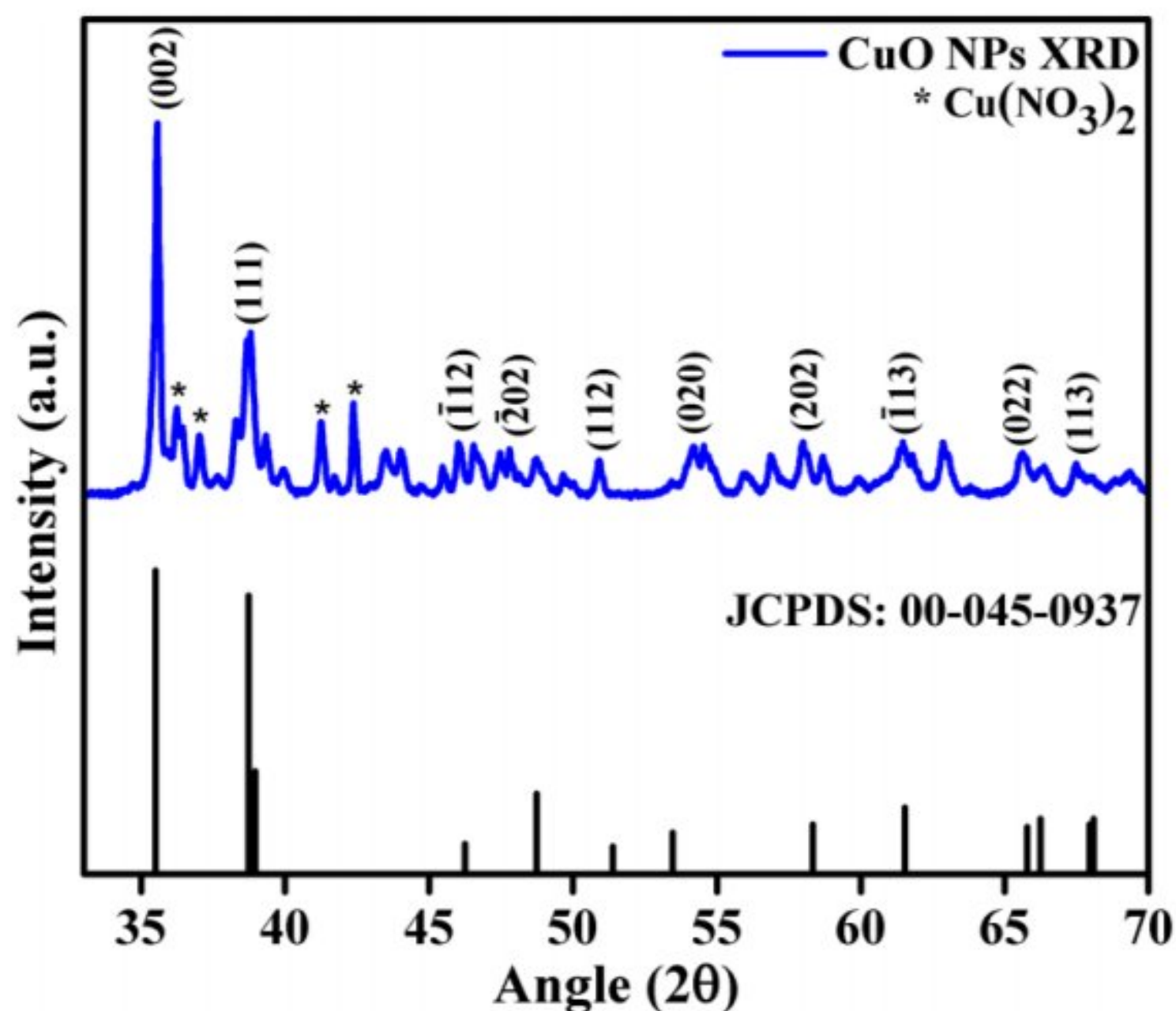


Figure 2. X-ray diffraction pattern with corresponding JCPDS file of the synthesized CuO nanoparticles.

### 3.2 Morphological Analysis

The structural analysis of synthesized CuO nanoparticles is done using FESEM. Figure 3 (a, b) shows the FESEM images of CuO nanoparticles acquired at 1  $\mu\text{m}$  and 200 nm magnifications. Figure 3(a) clearly shows the formation of distinct particles with uniformity over the complete surface, while Figure 3(b) shows the formation of cuboidal-shaped nanoparticles. As seen from the high magnification image it is concluded that all the cuboidal shaped nanoparticles are arranged to form ball-like structures. The average particle size of synthesized particles calculated from a high magnification image is 135 nm.

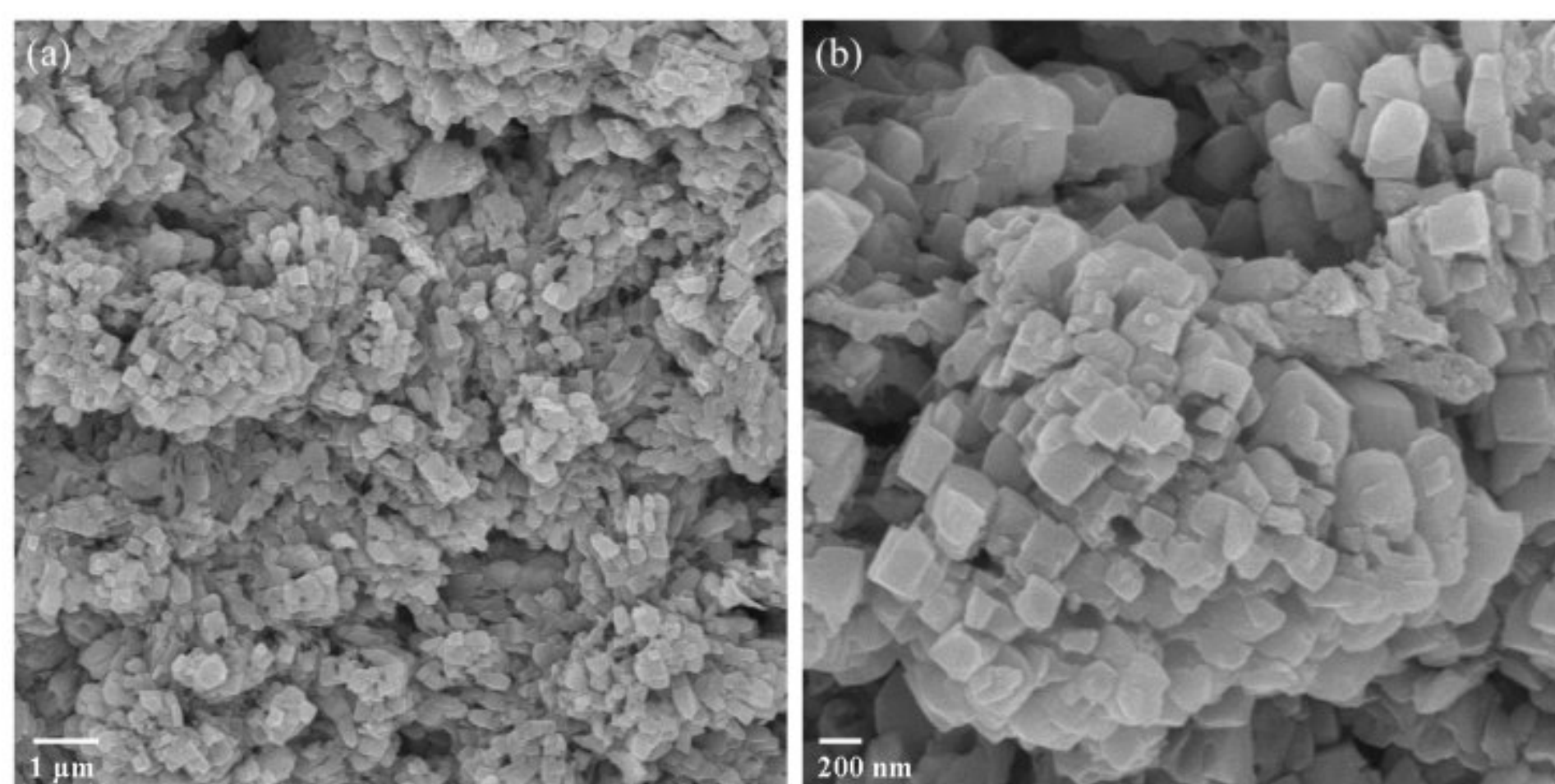


Figure 3. FESEM images of synthesized CuO nanoparticles at 1  $\mu\text{m}$  (a) and 200 nm (b).

### 3.3 FT-IR analysis

The most likely functional group included in the sample can be identified using FT-IR analysis [16]. Figure 4 displays the CuO nanoparticle's FT-IR spectrum. The Cu-O stretching vibrations of CuO nanoparticles can be seen from peaks at 746, 570 and 520  $\text{cm}^{-1}$  along different faces of monoclinic structure. The band maxima at 3398  $\text{cm}^{-1}$  and 3310  $\text{cm}^{-1}$  are indicative of adsorbed water molecules and are OH stretching vibration and HOH bending modes [16,17], respectively. The transmittance band at 1042, 846 and 815  $\text{cm}^{-1}$  can be connected to Cu-(OH), and C-O stretching vibrations of alcohol and phenolic-based compounds are denoted by peaks at 1491 and 1376  $\text{cm}^{-1}$  [18].

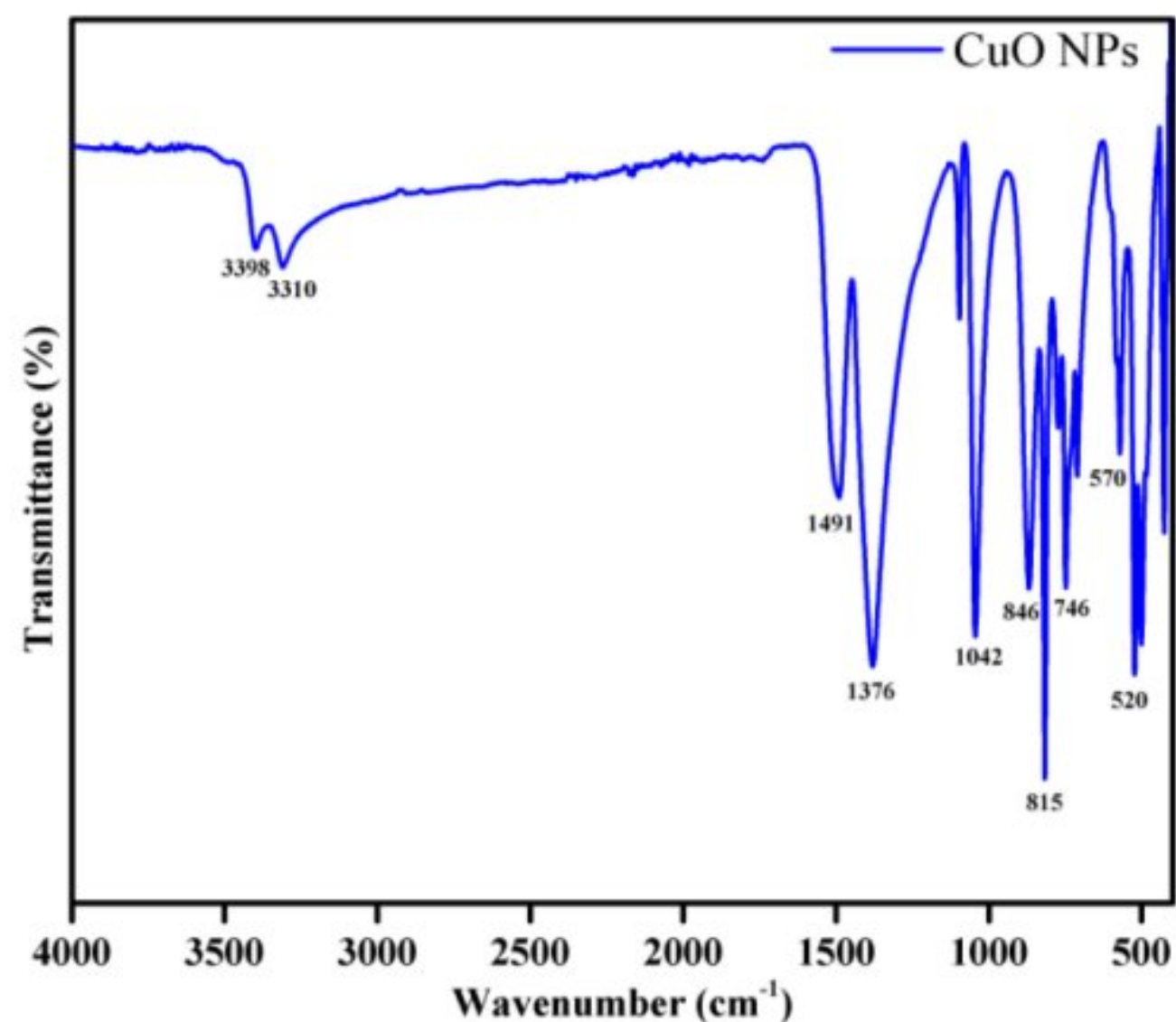


Figure 4. FTIR spectrum of CuO nanoparticles produced at 160°C.

### 3.4 EDX analysis

EDX is performed for the synthesized sample. The sample has an atomic weight percentage of 79.67 % of Cu and 12.50 % of O which can be seen from the EDX spectrum as shown in Figure 5. This shows that the synthesized sample contains Cu and oxygen in a ratio of 1.6:1 which confirms the formation of CuO nanoparticles. The extra peaks in EDX spectrum are inconsistency of the observed extra peaks in the XRD pattern of the sample.

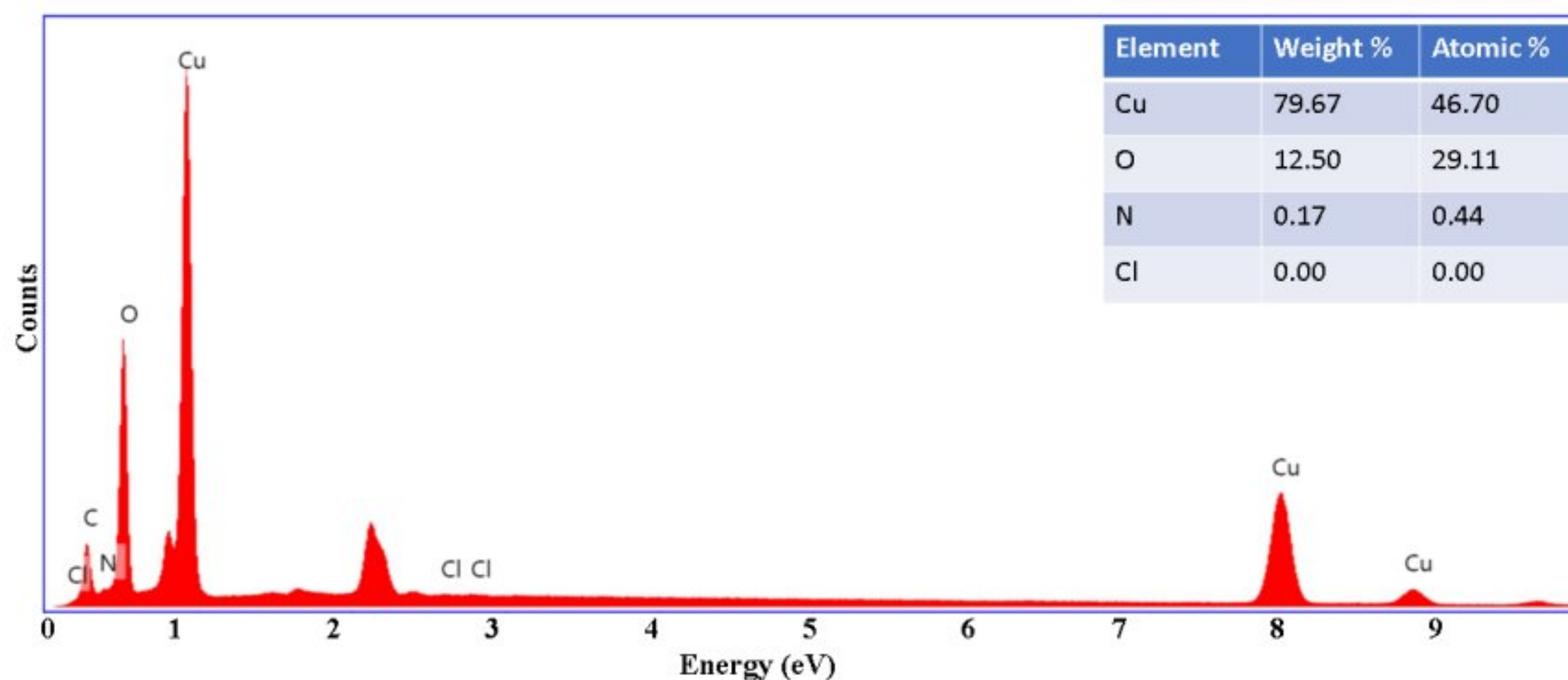


Figure 5. EDX spectrum of synthesized CuO nanoparticles and composition table (inset).

### 3.5 Photoluminescence analysis

Figure 6 displays the photoluminescence (PL) spectrum of CuO synthesized nanoparticles with an excitation of 320 nm at room temperature. A distinct PL band is detected at 417 nm. The broad PL can be related to vacancies and defects created by non-stoichiometric CuO. The shape, size, and excitation wavelength of the particles are thought to have a significant influence on the oxide material's emission wavelength [19]. The PL peak at 417 nm is commonly known as the near band edge emission or exciton emissions [20,21]. The presence of Cu vacancies in CuO causes non-stoichiometry [22].

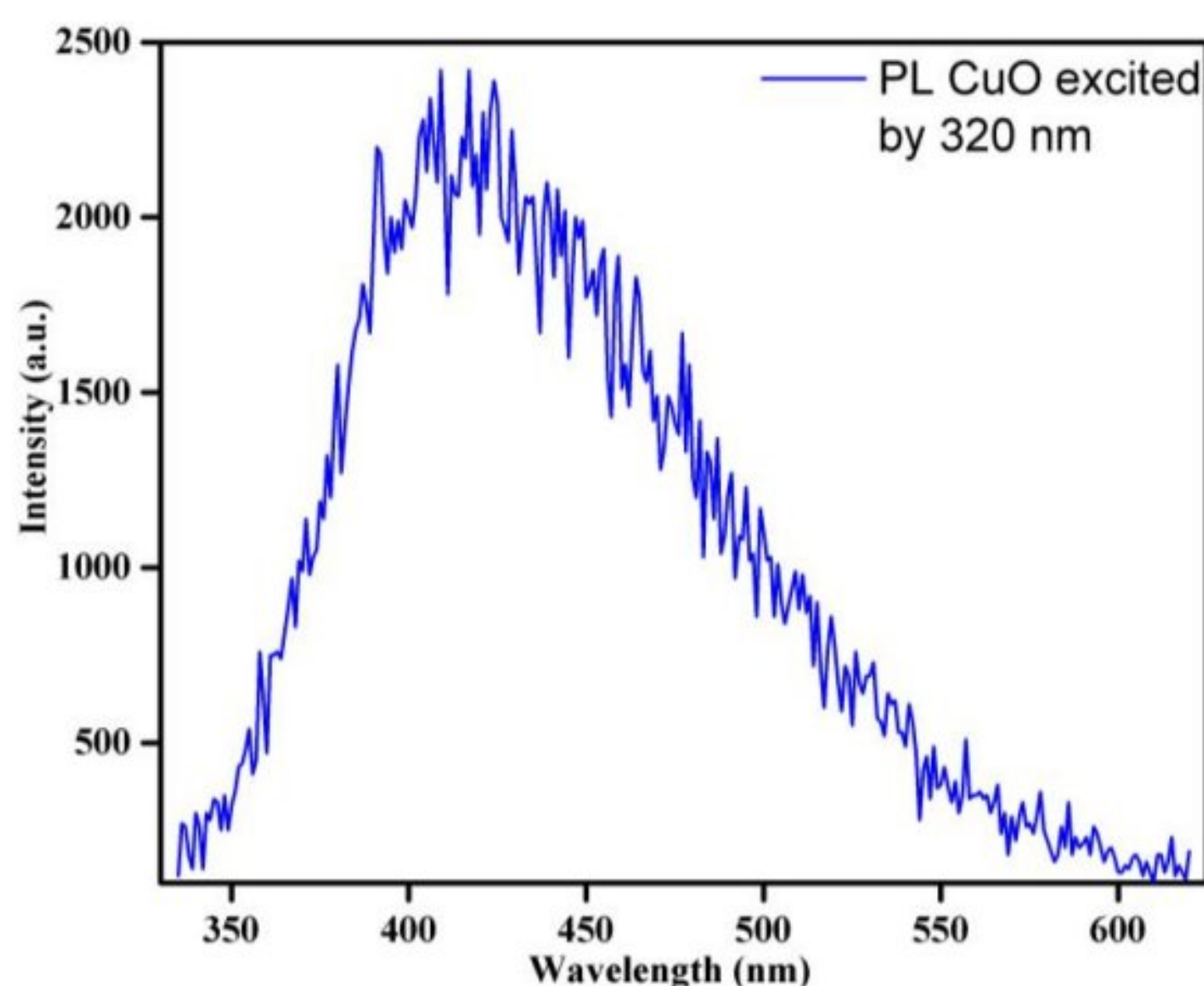


Figure 6. Photoluminescence spectrum of CuO nanoparticles.

### 4. Application as Acetone gas sensor

Acetone is a colourless liquid having a boiling point of 56.5 °C, melting point of 94 °C, density of 0.788 gram/cm<sup>3</sup> and a pungent characteristic smell [23]. It is commonly used in laboratories and industries to dehydrate tissues, purify paraffin and dissolve plastic. Acetone inhalation is harmful to health as it can lead to irritation in nose, throat and eyes as well. In high concentrations, it can lead to nausea, dizziness, drowsiness and headache

also [23]. So, the concentration of acetone needs to be monitored. CuO nanoparticles play an important role in acetone concentration detection. CuO particles high surface-to-volume ratio allows gas molecules to adsorb on their surface, which leads to extraordinary changes in the electrical characteristics of nanoparticles. The interaction between the pre-adsorbed oxygen on CuO and acetone gas is source of the CuO particle sensing mechanism. Pre-adsorbed oxygen may interact with CuO through charge exchange to create  $O^-$ . When CuO is exposed to acetone which is reductive in nature and pre-adsorbed oxygen there occurs a reaction between them. The majority carrier in p-type CuO is neutralised and free electrons are released via the reactions between the pre-adsorbed  $O^-$  and the acetone molecules. As a result of this change, there are less holes in CuO, which raises sensor resistance. As the acetone concentration is lowered, the amount of oxygen adsorbed on the CuO surface increases. This leads to lowering the sensor resistance towards the original stable state of CuO. For this, the concentration of acetone is taken as 100 ppm to 50 ppm. The gas sensing experiment was done at a temperature of 300 °C. The obtained resistance versus time graph is shown in Figure 7. The plot shows the responses of acetone for 6 different cycles of acetone sensing. The decrease in the peak maxima is due to the decrease in the concentration of acetone. According to the graph it can be clearly seen that the sample has a very low response and recovery time. The sensor shows a response time of approximately 10 sec and a recovery time of about 30 sec as calculated for 100 ppm concentration. Using the sensitivity formula calculation, it can be seen that the sample shows good sensitivity. As it can be seen from the plot, the resistance increases from 15K Ohmic resistance to about 500K Ohmic resistance on exposure to acetone. The value of sensitivity now can be calculated from Equations 1 as

$$\text{Sensitivity } (S) = \frac{500K}{15K} = 33.33 \quad (5)$$

Thus, a sensitivity of 33.33 is observed which shows that CuO is a good volatile gas sensor for gases like acetone.

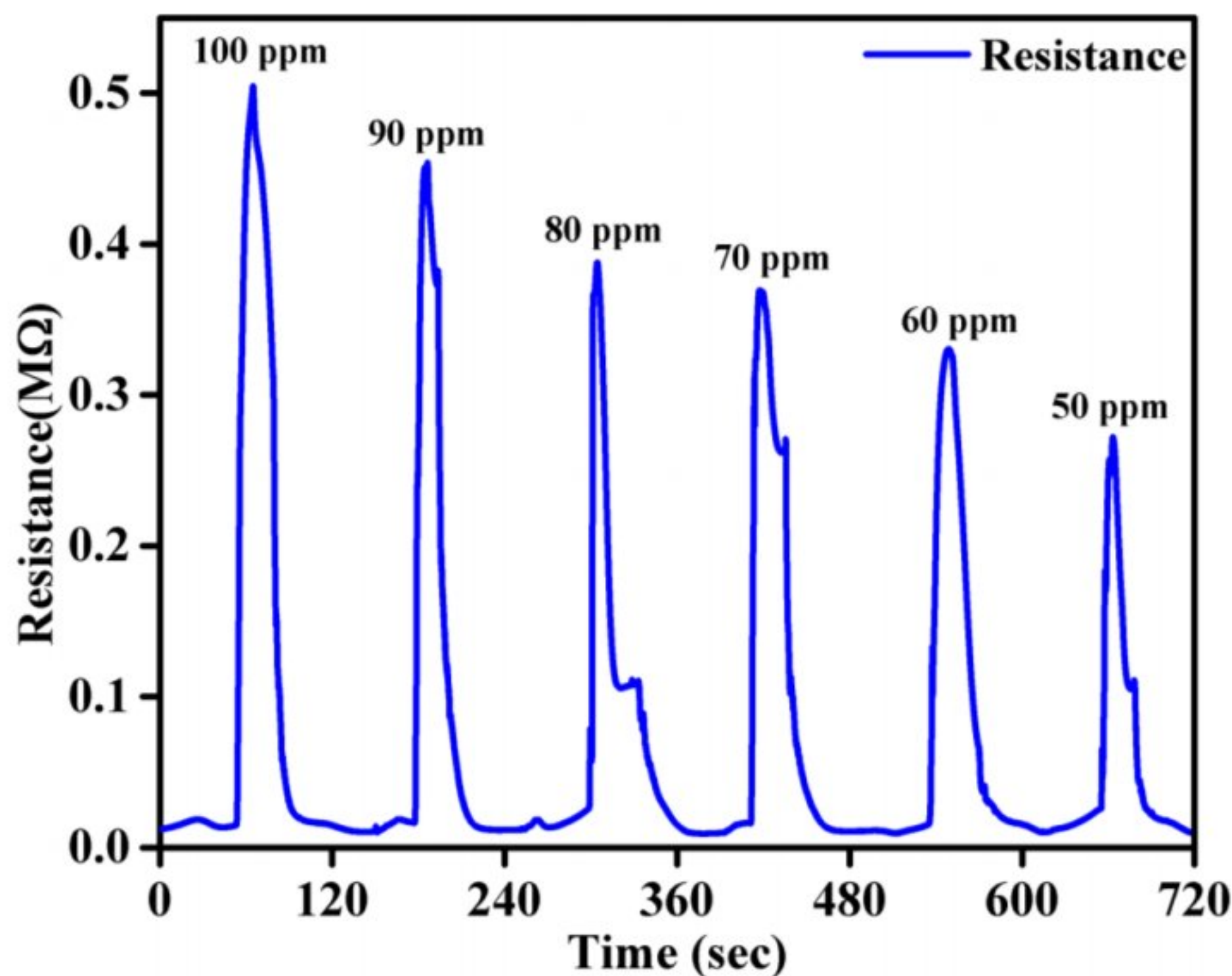


Figure 7. Variation of resistance (Ohm) with time for different cycles. Response recovery plot of CuO as acetone gas sensor at 300 °C.

## 5. Conclusions

In the present work, the successful synthesis of CuO nanoparticles is done without using any surfactant via a cost-effective hydrothermal method. Various characterizations are performed to validate the successful synthesis of CuO nanoparticles. The formation of cuboidal-shaped nanoparticles is confirmed by FESEM analysis. Phase and lattice parameters analysis is also done using the XRD method. Crystallite size is calculated for the most intense peak, which is found to be 44 nm. EDX analysis is used to check the composition of Cu and O and FTIR is performed to detect the presence of functional groups in synthesized sample. EDX confirmed formation of CuO nanoparticles in stoichiometry with some impurities of copper nitrate. FTIR confirmed the presence of

Cu-O bonds in the sample. Photoluminescence analysis is also performed which is used to confirm the presence of defects in the sample. Further, gas sensing properties of CuO nanoparticles were studied, sample showed a sensitivity of 33.33 for acetone gas which depicts CuO as a low cost and highly efficient sensor for sensing volatile gases like acetone.

### **Acknowledgement**

The authors are also thankful to the members of Laser and Spectroscopy lab, Applied Physics Department DTU for their kind help and support in carrying out the research work.

### **References**

1. K. Kumar and A. Chowdhury, *Ceram Int* **43**, 13943 (2017).
2. F. S. Ke, L. Huang, G. Z. Wei, L. J. Xue, J. T. Li, B. Zhang, S. R. Chen, X. Y. Fan, and S. G. Sun, *Electrochim Acta* **54**, 5825 (2009).
3. S. Kumar, A. K. Ojha, D. Bhorolua, J. Das, A. Kumar, and A. Hazarika, *Physica B Condens Matter* **558**, 74 (2019).
4. Z. Yang, Q. Rong, T. Bao, M. Jiao, L. Mao, X. Xue, W. Wen, Z. Wu, X. Zhang, and S. Wang, *Anal Chim Acta* **1199**, 339598 (2022).
5. N. Kumar, S. S. Parui, S. Limbu, D. K. Mahato, N. Tiwari, and R. N. Chauhan, *Mater Today Proc* **41**, 237 (2021).
6. G. K. Dalapati, R. S. Kajen, S. Masudy-Panah, and P. Sonar, *J Phys D Appl Phys* **48**, 495104 (2015).
7. G. Chaloeipote, R. Prathumwan, K. Subannajui, A. Wisitsoraat, and C. Wongchoosuk, *Mater Sci Semicond Process* **123**, 105546 (2021).
8. Y. Keriti, R. Brahim, Y. Gabes, S. Kaci, and M. Trari, *Solar Energy* **206**, 787 (2020).
9. M. Sreekanth, P. Srivastava, and S. Ghosh, *Appl Surf Sci* **508**, 145215 (2020).
10. T. Jiang, Y. Wang, D. Meng, X. Wu, J. Wang, and J. Chen, *Appl Surf Sci* **311**, 602 (2014).
11. C. C. Vidyasagar, Y. A. Naik, T. G. Venkatesh, and R. Viswanatha, *Powder Technol* **214**, 337 (2011).



12. N. Kumar, S. S. Parui, S. Limbu, D. K. Mahato, N. Tiwari, and R. N. Chauhan, *Mater Today Proc* **41**, 237 (2021).
13. T. Koh, E. O'Hara, and M. J. Gordon, *J Cryst Growth* **363**, 69 (2013).
14. R. Mohassel, F. Soofivand, Y. J. BahrAluloom, M. K. Imran, M. Shabani-Nooshabadi, and M. Salavati-Niasari, *Int J Hydrogen Energy* **48**, 10955 (2023).
15. M. Bin Mobarak, M. S. Hossain, F. Chowdhury, and S. Ahmed, *Arabian Journal of Chemistry* **15**, 104117 (2022).
16. A. Kathiravan and R. Renganathan, *J Colloid Interface Sci* **335**, 196 (2009).
17. J. Wei, L. Zhao, S. Peng, J. Shi, Z. Liu, and W. Wen, *J Solgel Sci Technol* **47**, 311 (2008).
18. V. Anto Feradrick Samson, K. Mohamed Racik, S. Prathapa, J. Madhavan, and M. Victor Antony Raj, *Mater Today Proc* **8**, 386 (2019).
19. J. Wan, L. Shi, B. Benson, M. J. Bruzek, J. E. Anthony, P. J. Sinko, R. K. Prudhomme, and H. A. Stone, *Langmuir* **28**, 13143 (2012).
20. E. Velázquez Lozada, G. M. Camacho González, and T. Torchynska, *J Phys Conf Ser* **582**, (2015).
21. S. Dagher, Y. Haik, A. I. Ayes, and N. Tit, *J Lumin* **151**, 149 (2014).
22. K. Srinivasa Rao and T. Vanaja, *Mater Today Proc* **2**, 3743 (2015).
23. A. Mirzaei, S. G. Leonardi, and G. Neri, *Ceram Int* **42**, 15119 (2016).